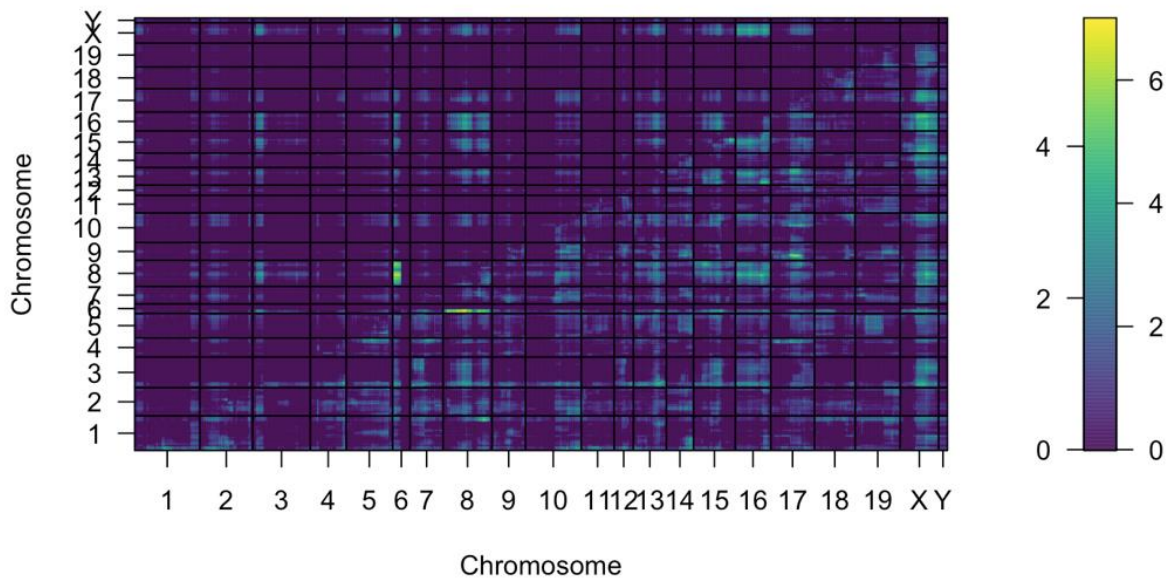


Supplemental material

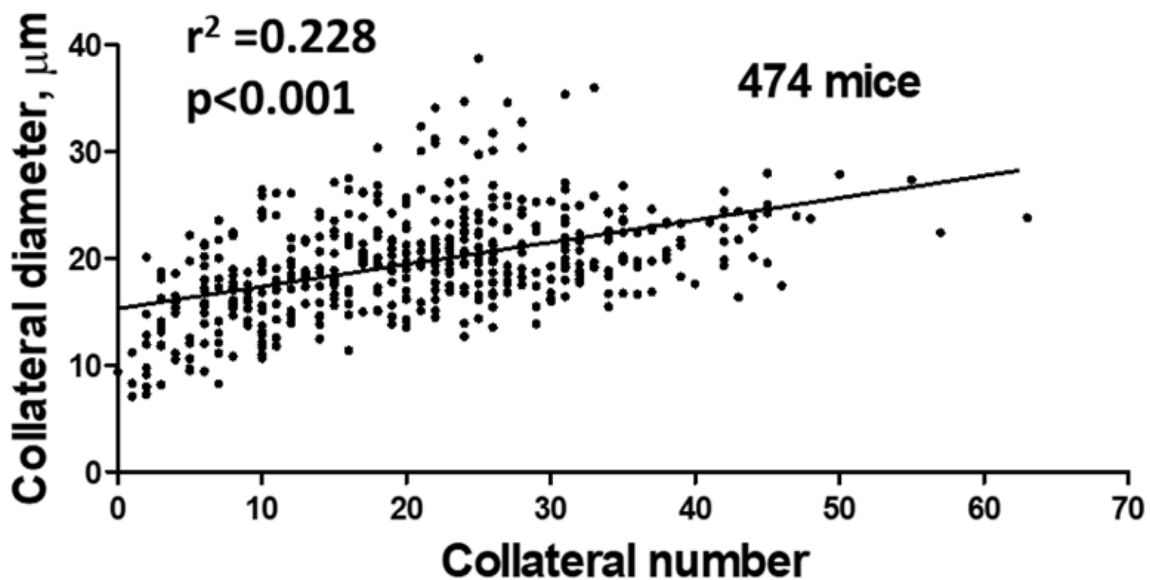
Large differences in collateral blood vessel abundance among individuals arise from multiple genetic variants

James E Faber, Hua Zhang, James G Xenakis, Timothy A Bell, Pablo Hock, Fernando Pardo-Manuel de Villena, Martin T Ferris, Wojciech Rzechorzek

1. Supplemental figure I. *Canq5* and *Canq6* exhibit additive independent effects.
2. Supplemental figure II. Collateral diameter weakly correlates with collateral number in 60 Collaborative Cross strains.
3. Supplemental data for QTL for collateral number with LOD > 4.5 shown in Figure 3.
4. Supplemental figure III. In vivo analysis of candidate genes for effect on collateral diameter.
5. Supplemental table I. Characteristics of QTL for variation in collateral number.
6. Supplemental table II. Genes underlying *Canq5*-to-*Canq10* with SNP(s) in the haplotype block of the high-collateral strains in the crosses shown in Table 1.
7. Supplemental table III. Genes within ± 10 Mb of QTL peak that lack nonsense or missense SNPs but have functions known to be involved in or associated with collaterogenesis (a), angiogenesis (b), vascular development (c), endothelial cell function (d), or endocytic vesicle trafficking (e).
8. Supplemental table IV. Coding and nonsense variants present in human orthologs of mouse genes known to (“Known genes”) and “Candidate genes” predicted to impair collaterogenesis.
9. Bioinformatics analysis of candidate genes’ function, expression, and potential involvement in the collaterogenesis pathway.
10. Possible signaling pathways for the genes listed in “Bioinformatic analysis” and Supplemental table IV, plus selected genes listed in Supplemental table III



Supplemental figure I. Supplemental Figure 2: Two-QTL scan for CC036xCC055. To investigate possible pairwise joint effects of QTL, we performed a two-dimensional, two-QTL genome scan using the function `scantwo()` in R/qtl. In this plot, the marginal improvement in LOD score from the two QTL models with interactions versus null models with no QTL are visualized in the lower right triangle. The marginal improvements in LOD score from the full two-QTL models with interactions versus additive two-QTL models without interactions are visualized in the upper left triangle. This plot provides evidence for the additive effects of most loci in these models, and some evidence for an interactive effect between the QTL on chromosomes 6 and 8.



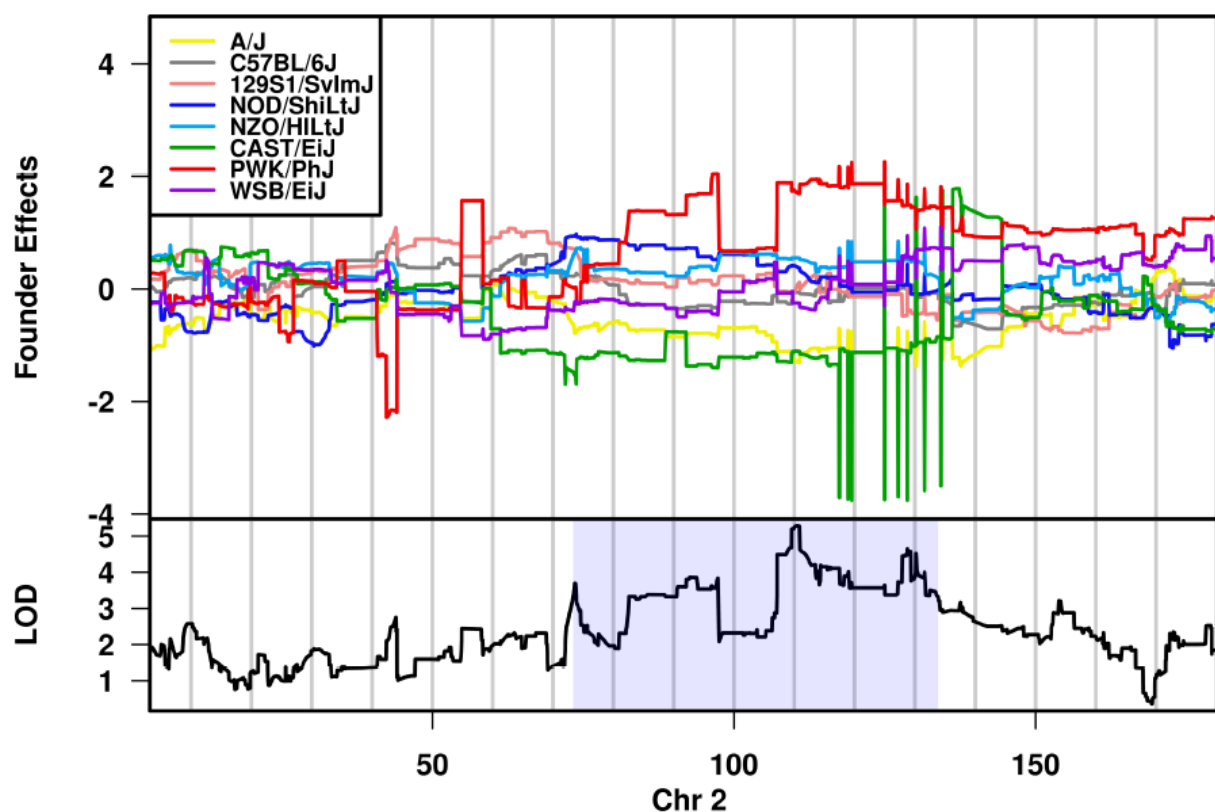
Supplemental figure II. Collateral diameter weakly correlates with collateral number in 60 CC strains. Data are taken from Figure 1. The low coefficient of determination for the 3.4-fold range in diameter and 47-fold range in number across the 60 CC strains shown in Figure 1 is consistent with previous findings (see Results and Discussion).

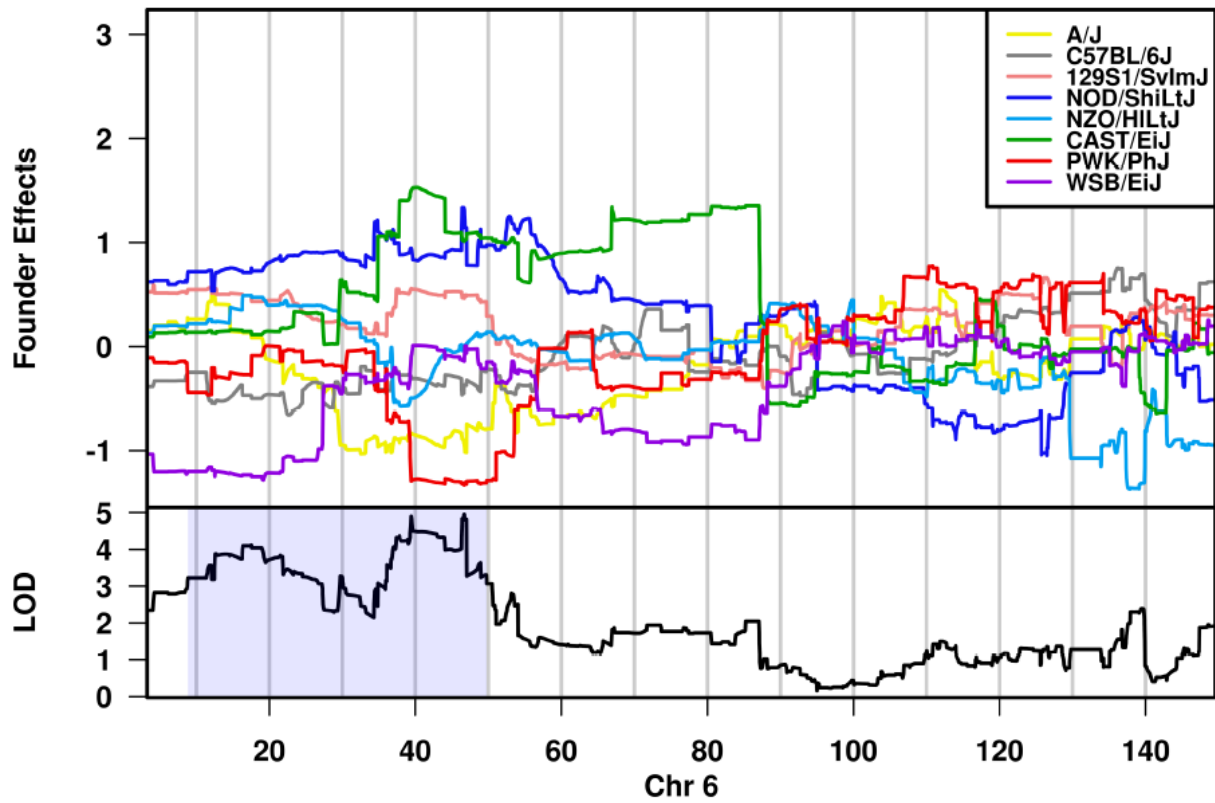
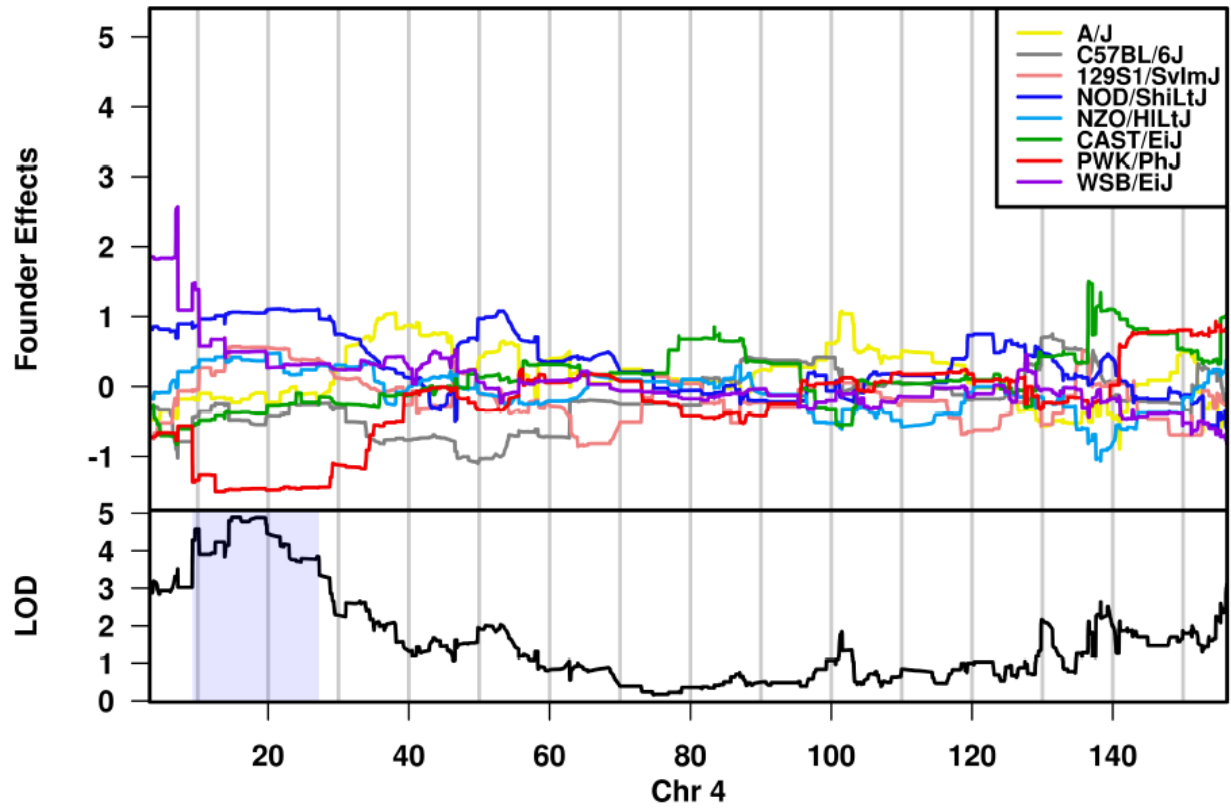
Data for QTL for collateral number with LOD > 4.5 shown in Figure 3

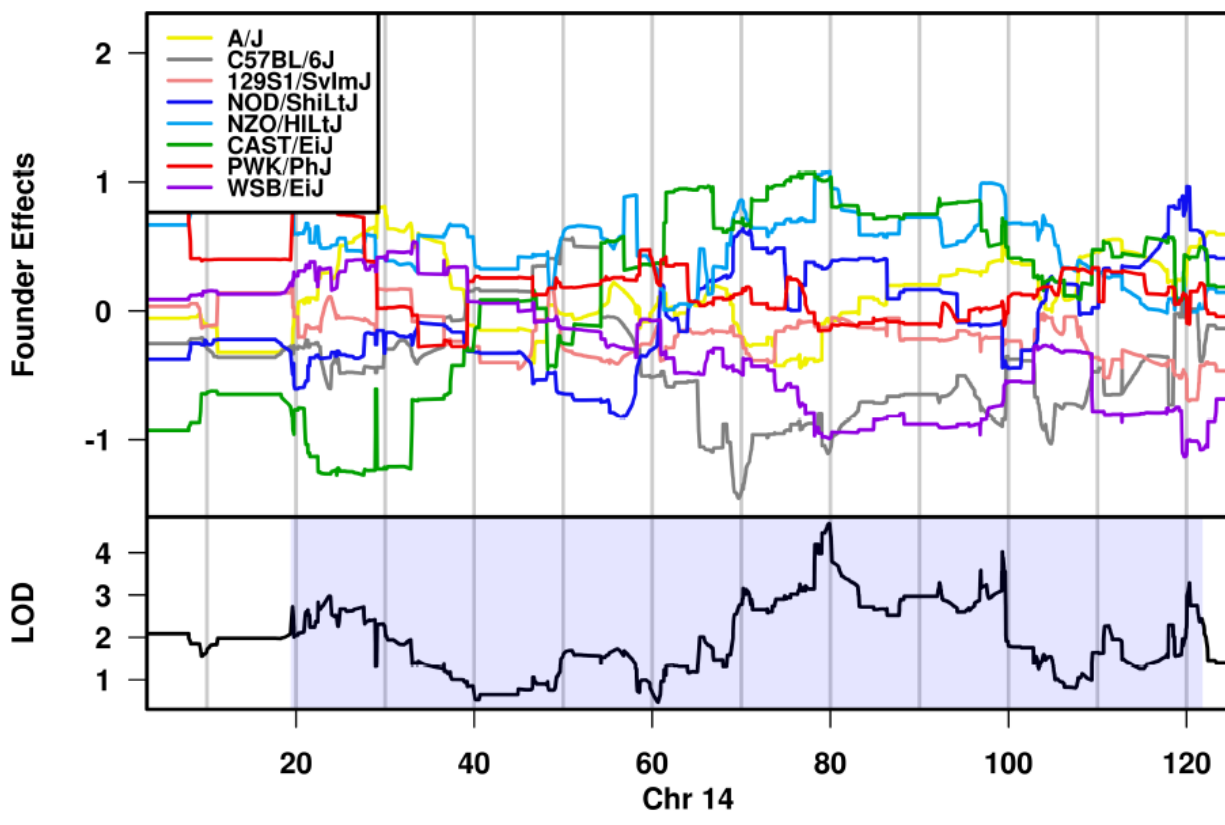
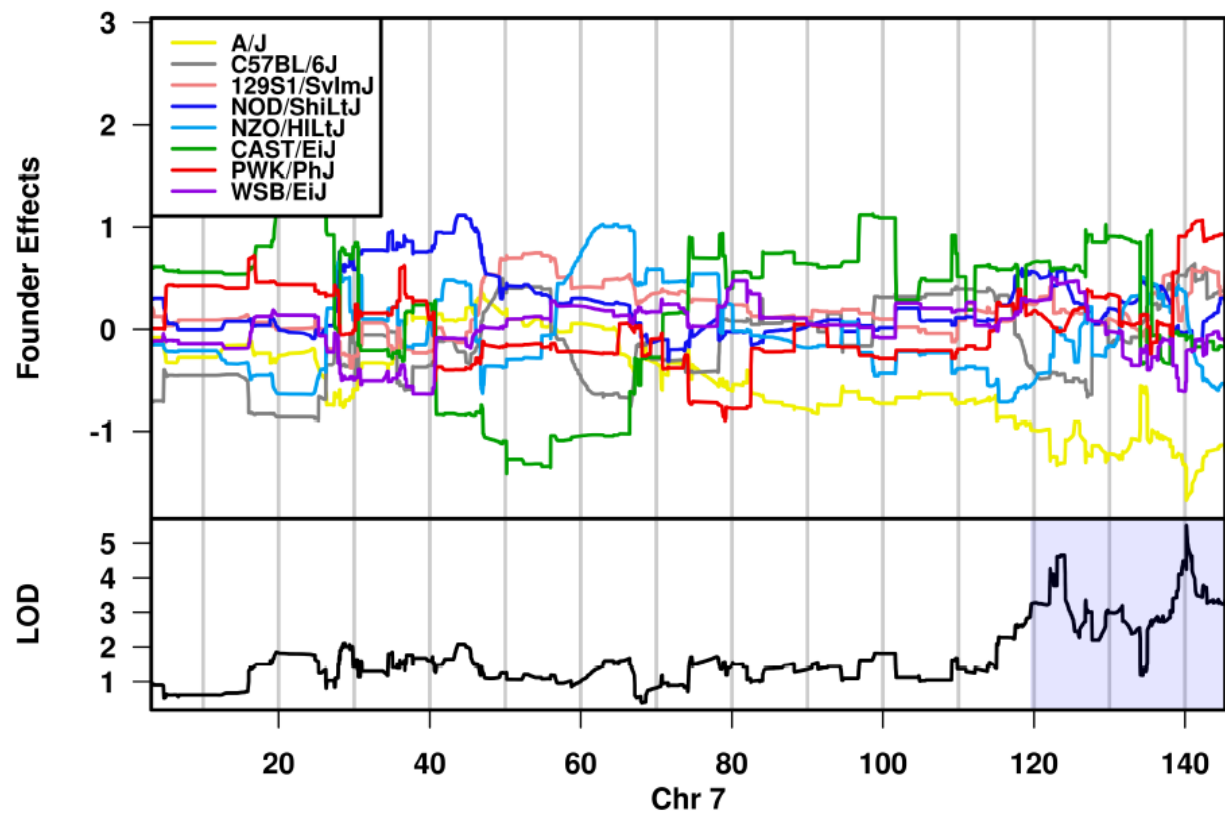
Chr	Marker	Position (Mb)	LOD	P-value	% variation	Proximal(Mb)	Distal (Mb)
2	UNC3746900	110.517931	5.28	0.0010	34.25	73.3	136.5
4	UNC6795401	15.990326	4.89	0.0021	32.18	9.3	26.9
6	UNC11014318	46.699174	4.95	0.0019	32.50	8.9	50.0
7	UNC13997623	140.182648	5.50	0.0007	35.40	119.5	145.3
14	UNC24324427	79.868383	4.68	0.0030	31.05	19.4	121.5
19	UNC30423453	48.179191	4.90	0.0020	32.23	33.0	58.2

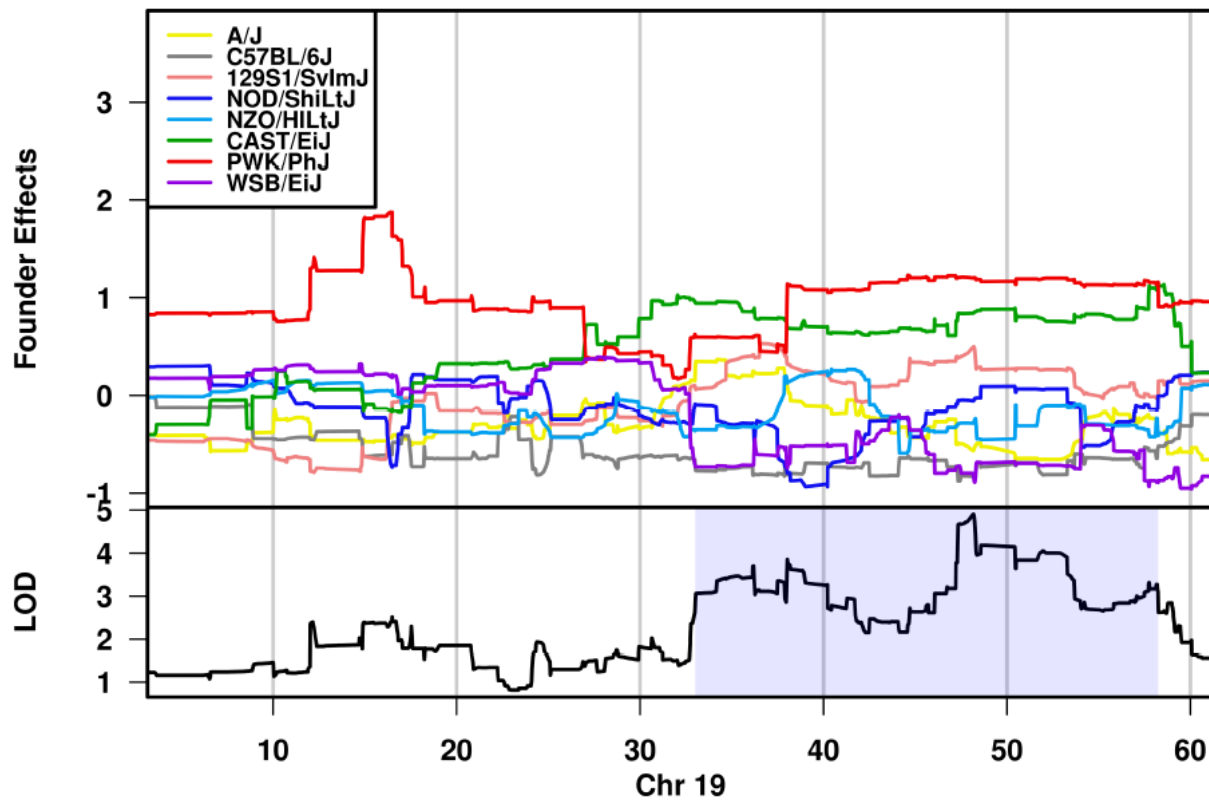
The data given above and below were obtained using gQTL v1.6 (1/2019; developed by Dr. Kranti Konganti, Texas A&M University). Chr, chromosome; Marker, Position, marker SNP and peak location on chromosome; P values are based on 1000 permutations.

The below figures show the founder effects for the above QTL.

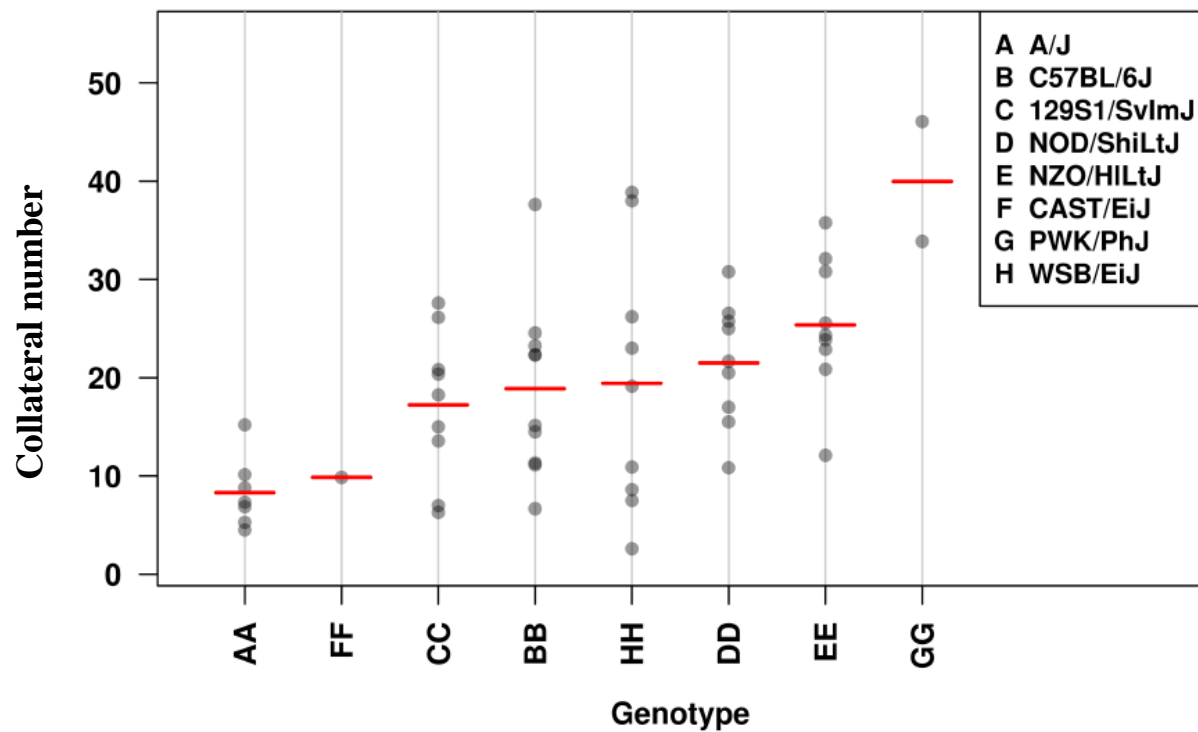




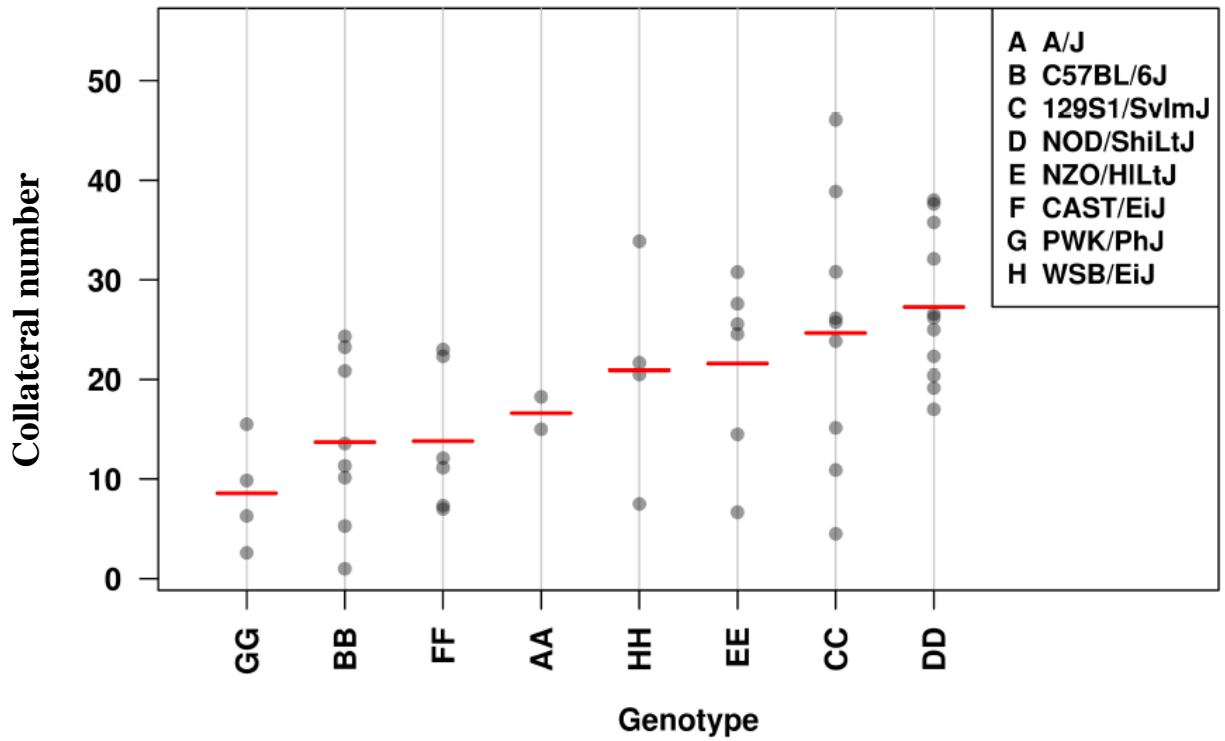




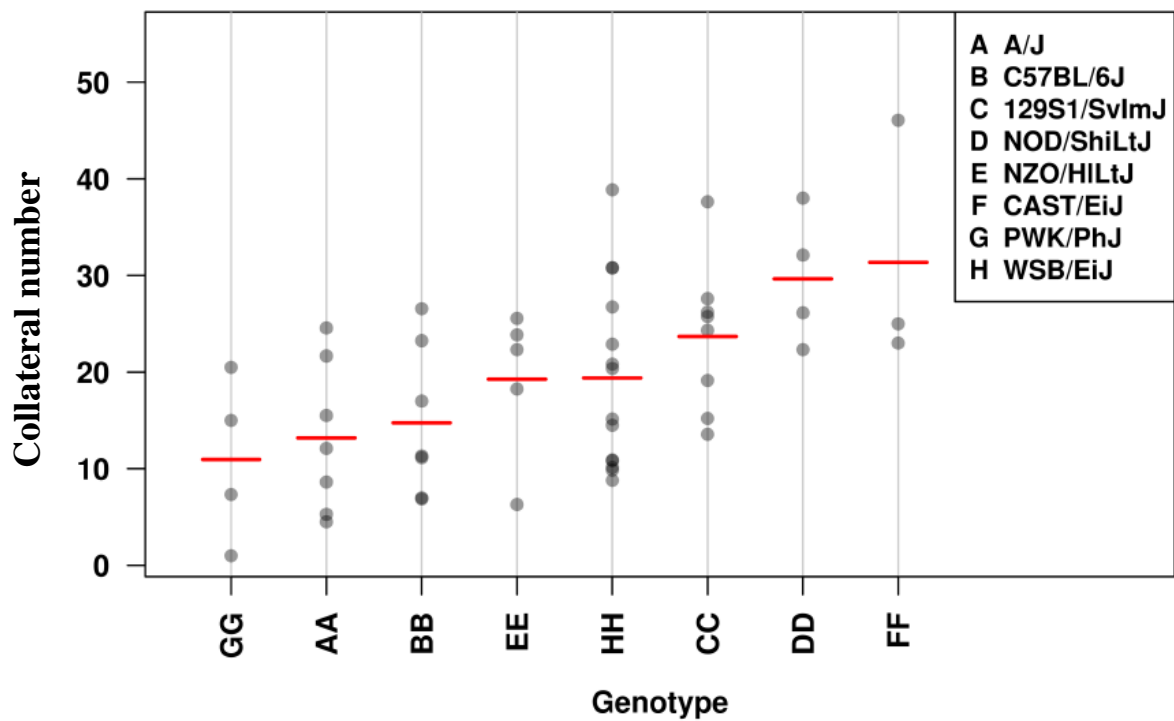
UNC3746900
Chr 2 : 110517931 Mb



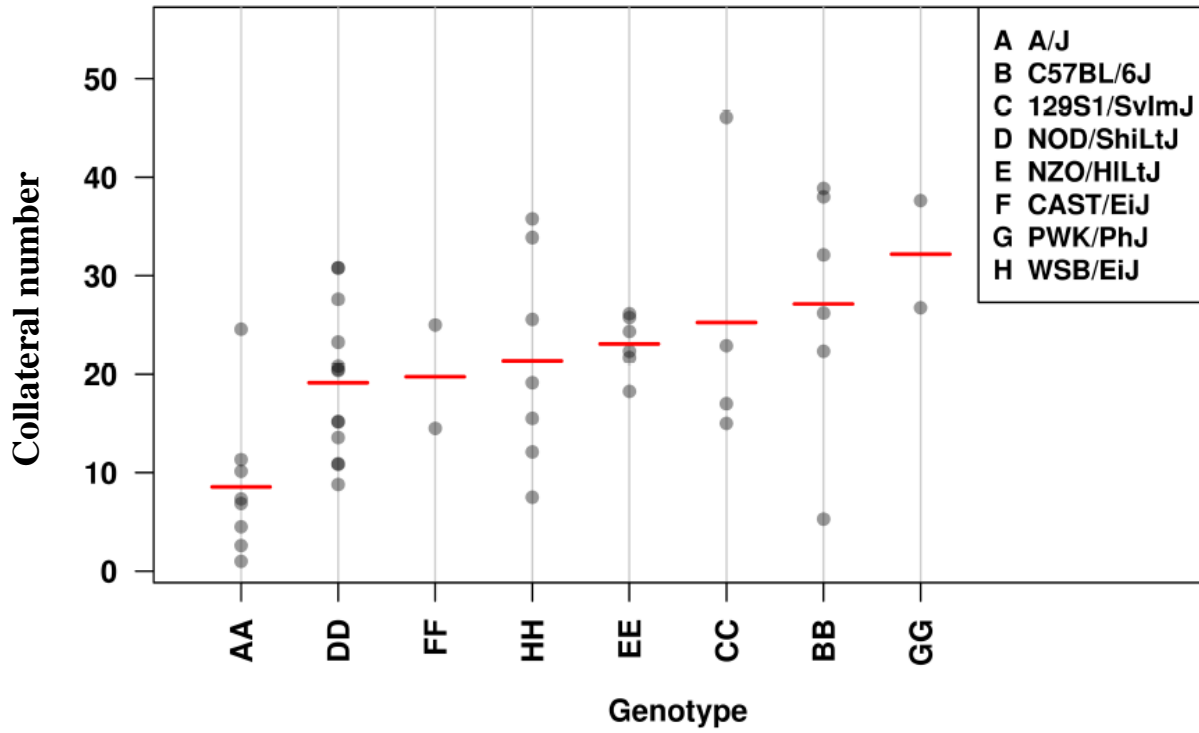
UNC6795401
Chr 4 : 15990326 Mb



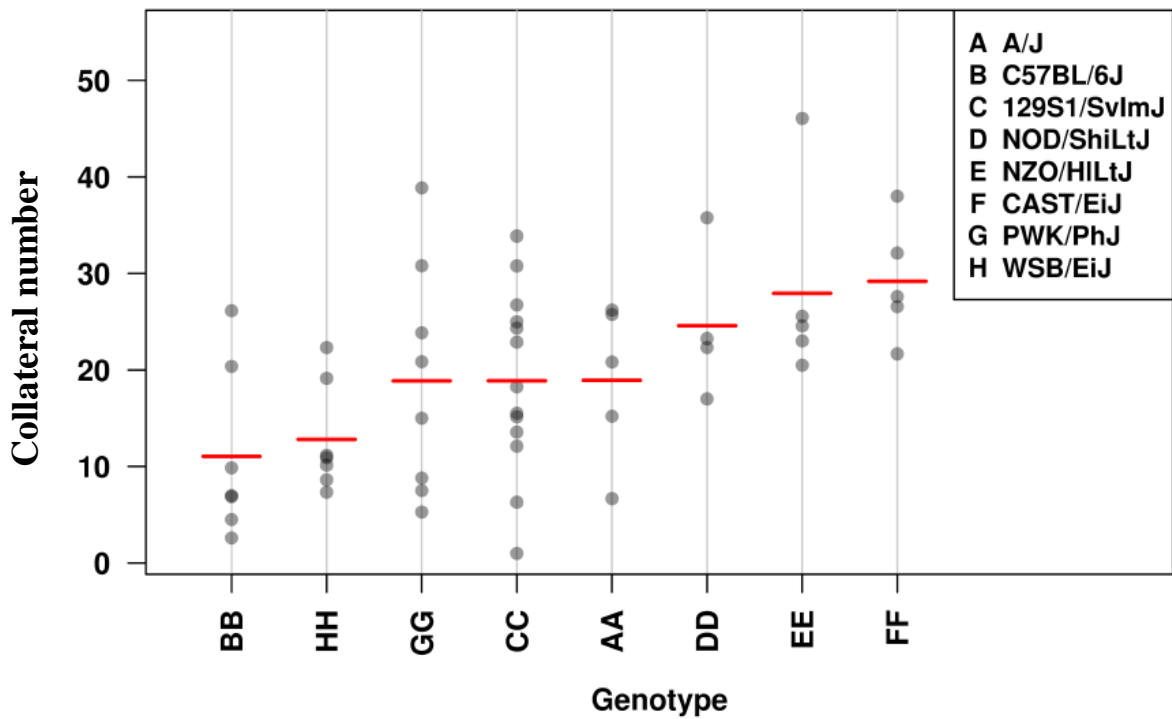
UNC11014318
Chr 6 : 46699174 Mb



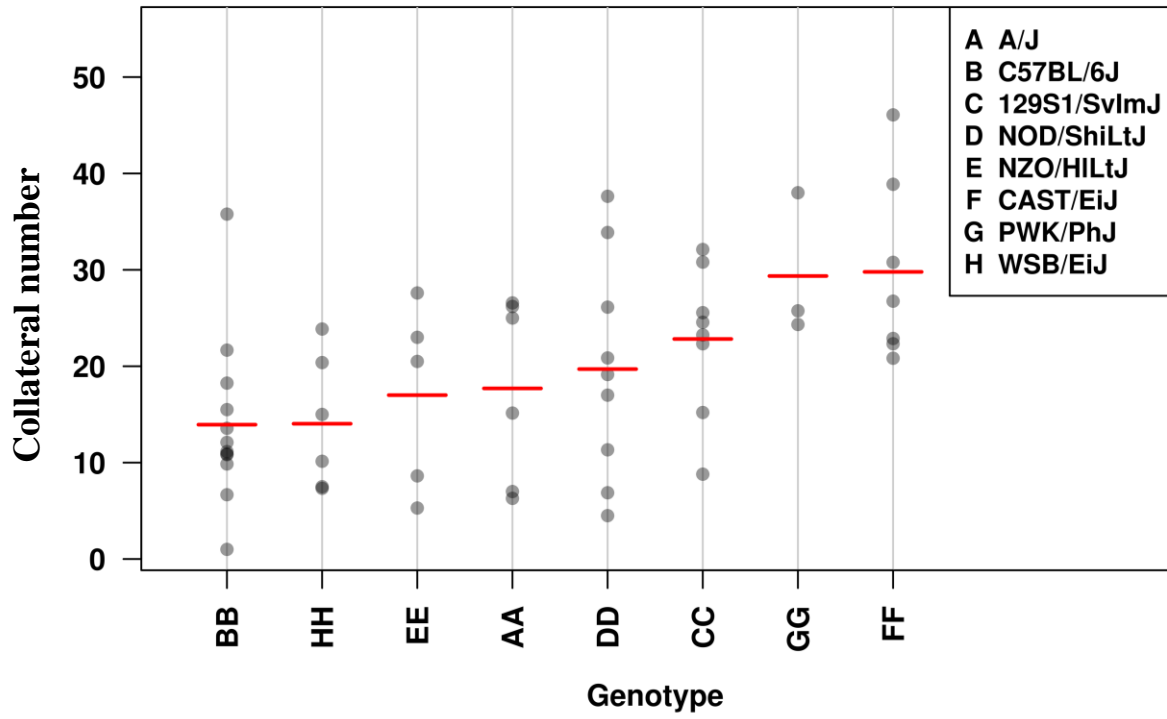
UNC13997623
Chr 7 : 140182648 Mb

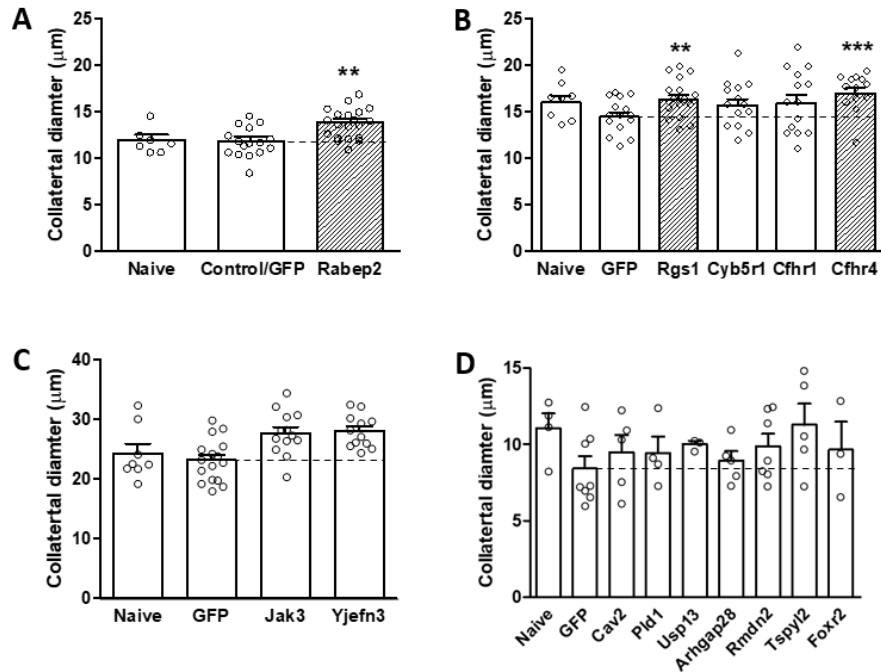


UNC24324427
Chr 14 : 79868383 Mb



UNC30423453
Chr 19 : 48179191 Mb





Supplemental figure III. In vivo analysis of candidate genes for effect on collateral diameter. AAV9-expression constructs for *Rabep2* (panel A) and selected high-priority candidate genes underlying *Canq5* (B), *Canq6* (C) and *Canq7-10* (D) were injected iv on postnatal day-zero before blood brain barrier closure into *Rabep2*^{-/-} (A), CC016 (B), CC032 (C) and CC036 (D) mice. Average diameter for all collaterals between the MCA and ACA trees of both hemispheres was measured for each mouse at 6 weeks-age. Naive, no injection; Control/GFP, injection of AAV9 construct for enhanced green fluorescent protein only. Number of animals for each bar: Panel A: 7,16,20; B: 8,15,17,14,14,13; C: 8,16,13,12; D: 4,8,5,4,3,5,7,5,3 (smaller n-sizes than in Figure 6D reflect animals with no collaterals). *p<0.05, ***p<0.001 vs. Control/GFP by 1-sided *t*-tests.

Supplemental table I. Characteristics of QTL for variation in collateral number

Cross	QTL	Chr	Marker	Position	LOD, P-value	Interval (M)	Haplotype blocks
049 x 053	<i>Canq5</i>	1	gUNC1733690	135,464,050	10.88 <0.001	127.48-157.13	WSB high, A/J low
055 x 036	<i>Canq6</i>	8	mJAX00671437	68,343,478	10.39 <0.001	55.82-78.90	129S1 high, C57 low
055 x 036	<i>Canq7</i>	6	gJAX00603740	15,909,737	6.90 <0.001	4.03-26.49	CAST high, WSB low
055 x 036	<i>Canq8</i>	3	mUNC4993850	32,940,787	5.79 <0.001	29.47-45.57	CAST high, A/J low
055 x 036	<i>Canq9</i>	17	UNC28266829	70,113,081	5.84 <0.001	60.00-80.94	A/J high, WSB low
055 x 036	<i>Canq10</i>	X	gUNC31504684	157,934,381	5.85 <0.001	141.50-164.42	PWK high, 129S1 low
055 x 036	<i>Canq11</i>	13	mUNC130149286	85,808,377	4.78 0.008	3.56-109.60	
055 x 036	<i>Canq12</i>	16	mUNC26808608	50,710,699	5.08 0.004	25.09-95.80	

Cross, parental CC strains; Chr, chromosome; Marker, Position, marker SNP and peak location on chromosome; 95% confidence interval, Haplotype blocks: “high” denotes haplotype block harboring locus for high collateral number (protective allele) in CC049 or CC055, “low” denotes haplotype block harboring locus for low collateral number (deleterious allele) in CC053 or CC036. P values are based on 1000 permutations.

Supplemental table II. Genes underlying *Canq5*-to-*Canq10* with SNP(s) in the haplotype block of the high-collateral strains in the crosses shown in Figure 4A.

Locus	Symbol	Description	RS number	Coding change	Allele	P-value for deleterious effect		
						SIFT	SIFT-P	PROV*
<i>Canq5</i>								
	<i>Igfn1</i>	immunoglobulin-like and fibronectin type III domain containing 1	rs30911401	P607S	W	0.020	0.012	-4.43
			rs253370915 ^a	S633P	W	0.030	0.001	-1.89
	<i>Crb1</i>	crumbs family member 1	rs30924175	P269L	W	0.000	0.002	-8.50
	<i>Cacna1s</i>	calcium channel, voltage-dependent, L type, alpha 1S subunit	rs223895038	P3L	W	0.000	0.000	-1.30
	<i>Il19</i>	interleukin 19	rs33497741	S105I	W	0.000	0.003	-3.82
			rs33495994	T8P	W	0.020	0.014	-0.82
	<i>Kif14</i>	kinesin family member 14	rs238546255	E426G	W	0.010	0.090	-3.31
	<i>Emk2</i>	ethanolamine kinase 2	133,365,816 ^b	Stop	W			
	<i>Ppp1r15b</i>	protein phosphatase 1, regulatory subunit 15B	rs33493063	P398S	W	0.020	0.002	-2.84
	<i>Cntn2</i>	contactin 2	rs36402706	R64H	W	0.000	0.002	-2.54
	<i>Lax1</i>	lymphocyte transmembrane adaptor 1	rs32582773	P67S	W	0.080	0.048	-6.72
	<i>Pigr</i>	polymeric immunoglobulin receptor	rs241665934	P607S	W	0.010	0.030	-2.86
			rs30820548	T39M	W	0.060	0.030	-1.08
	<i>Thsd7b</i>	thrombospondin, type I, domain containing 7B	rs264931691	R1154Q	W	0.020	0.001	-2.73
	<i>Acmsd</i>	amino carboxymuconate semialdehyde decarboxylase	rs46700071	T69I	W	0.020	0.012	-3.65
	<i>Zranb3</i>	zinc finger, RAN-binding domain containing 3	rs222620320	R317C	W	0.010	0.027	-4.00
	<i>Lct</i>	Lactase	rs50723357	T939M	W	0.000	0.001	-2.40
	<i>Map3k19</i>	mitogen-activated protein kinase kinase kinase 19	rs46700071	T69I	W	0.020	0.012	-3.65
<i>Canq6</i>								
	<i>Nek1</i>	NIMA (never in mitosis gene a)-related expressed kinase 1	rs239230033	R39S	I	0.050	0.050	-2.71
	<i>Sh3rf</i>	SH3 domain containing ring finger 1	rs33135970	G84V	I	0.020	0.004	-3.84
	<i>Gdf1</i>	growth differentiation factor 1	rs32650885	S145C	I	0.020	0.014	-2.16
	<i>Prmt9</i>	protein arginine methyltransferase 9	rs45636255	Q824H	P	0.050	0.066	-1.59
	<i>Nwd1</i>	NACHT and WD repeat domain containing 1	rs237177178	Y1386C	P	0.010	0.020	-2.56
	<i>Sugp2</i>	SURP and G patch domain containing 2	rs32650665 ^c	Stop	I			
	<i>Zfp963</i>	zinc finger protein 963	rs33361474	S185N	I	0.050	0.038	-1.20
			rs32816029	E49K	I	0.030	0.027	-2.06
<i>Canq7</i>								
	<i>Tfec</i>	transcription factor EC (E-box containing)	rs37583912	R306Q	C	0.020	0.029	-2.75
			rs241258046	D9E	C	0.010	0.008	-0.01
	<i>Ppp1r3a</i>	protein phosphatase 1, regulatory subunit 3A	rs33469811	D870H	C	0.000	0.001	-2.02
	<i>Ptprz1</i>	protein tyrosine phosphatase, receptor type Z, polypeptide 1	rs240106830	L8F	C	0.000	0.002	-0.83
			rs33747302	L843P	C	0.030	0.040	-1.35
			rs33748034	T893A	C	0.010	0.070	-1.20
			rs33748042	A1181T	C	0.000	0.001	-0.05
	<i>Vwde</i>	Willebrand factor D and EGF domains	rs46632271	L9M	C	0.020	0.037	-0.34
	<i>Tmem168</i>	transmembrane protein 168	rs212279097	N332D	C	0.070	0.042	-0.45
	<i>Pot1a</i>	protection of telomeres 1A	rs226408196	V551I	C	0.030	0.033	-0.39
	<i>Ctnb2</i>	cortactin binding protein 2	rs36251448	P1213T	C	0.090	0.087	-1.52
<i>Canq8</i>								
	<i>Plk4</i>	polo like kinase 4	rs49839395	S601A	C	0.040	0.028	-2.37
	<i>Skil</i>	SKI-like	rs29841544	P367A	C	0.040	0.030	-1.32
			rs29814968	L463F	C	0.060	0.021	-1.15
	<i>Intu</i>	inturned planar cell polarity protein	rs255853181	R273W	C	0.010	0.011	-0.80
	<i>Actr3</i>	actin related protein T3	rs246289103	V149M	C	0.000	0.000	-2.56
	<i>Samd7</i>	sterile alpha motif domain containing 7	rs252671701	P45L	C	0.020	0.068	-0.86
			rs261109659	P140S	C	0.080	0.008	-4.47
	<i>Lrriq4</i>	leucine-rich repeats and IQ motif containing 4	rs253521416	I31N	C	0.010	0.003	-0.68
	<i>1810062G17Rik</i>	RIKEN cDNA 1810062G17 gene	rs259087812	Stop ^d	C			
	<i>Mfn1</i>	mitofusin 1	rs29864746	A641V	C	0.070	0.016	-1.91
	<i>Ccdc144b</i>	coiled-coil domain containing 144B	rs49535369	V68E	C	0.020	0.382	-1.52
	<i>Ccna2</i>	cyclin A2	rs229616401	A144D	C	0.030	0.011	0.78
<i>Canq9^e</i>								
	<i>Ndufa7</i>	NADH:ubiquinone oxidoreductase complex assembly factor 7	rs50621970	R336H	A	0.000	0.031	-3.59
<i>Canq10</i>								
	<i>Gja6</i>	gap junction protein, alpha 6	rs29305426	I283T	P	0.020	0.013	0.89
	<i>Wnk3</i>	WNK lysine deficient protein kinase 3	rs29293581	R725Q	P	0.000	0.000	-3.71
	<i>Scml2</i>	Scm polycomb group protein like 2	rs248836551	P628A	P	0.030	0.006	-2.20
	<i>Ofd1</i>	OFD1, centriole and centriolar satellite protein	rs31559944	F1010C	P	0.050	0.006	-1.91
	<i>Zrsr2</i>	zinc finger (CCCH type)	rs252840144	S424C	P	0.040	0.030	-2.45
	<i>Magea5^f</i>	MAGE family member A5	rs583713186	K185N	P	0.040	0.014	-4.63
	<i>Asb11</i>	ankyrin repeat and SOCS box-containing 11	rs31454203	Q3P	P	0.020	0.009	-0.21
	<i>Frrmp4</i>	FERM and PDZ domain containing 4	rs254540233	M42I	P	0.050	0.023	-0.57

<i>Cdkl5</i>	cyclin-dependent kinase-like 5	rs29305426	I283T	P	0.020	0.013	0.89
<i>Adgrg2</i>	adhesion G protein-coupled receptor G2	rs257666586	I670T	P	0.030	0.16	1.73
<i>Tro</i>	Trophinin	rs29297514	A1267G	P	0.000	-----	-0.93

Table lists the genes in the high-collateral strain, their SNP rs numbers, coding change, allele and P-values (See legend to Table 1 for additional information). A,W,C,B,1,P, abbreviations for strain-specific haplotype allele harboring SNP for, respectively: A/J, WSB/EiJ, CAST/EiJ, C57BL/6J, 129S1/SvImJ, PWK/PhJ. ^a, Five additional SNPs (W allele) are < 0.1 by SIFT, 3/5 < 0.05 by SIFT-P, 5/5 -0.21 to -2.24 by PROVEAN. ^b, Stop is in first of 8 exons. ^c, Stop at amino acid position 58 of 158. ^d, Stop at amino acid position 10 of 129. ^e, interval analysis was confined to -5 → +10 Mb due to haplotype heterozygosity. ^f, *Magea5* has a private missense snp (C/T) at location 155089004 that is predicted deleterious (p < 0.05).

Supplemental table III. Genes within ± 10 Mb of QTL peak that lack nonsense or missense SNPs but have functions known or potentially involved in collaterogenesis (a), angiogenesis (b), vascular development (c), endothelial cell function (d), or endocytic vesicle trafficking (e).

QTL	Symbol	Description
<i>Canq5</i>	<i>Cxcr4</i> ^{a,b,c,f}	chemokine (C-X-C motif) receptor 4
	<i>Atp2b4</i> ^{b,d}	ATPase, Ca ⁺⁺ transporting, plasma membrane 4
	<i>Optc</i> ^{b,d}	opticin
	<i>Cfh</i> ^{b,d}	complement component factor h
	<i>Pik3c2b</i> ^e	phosphatidylinositol-4-phosphate 3-kinase catalytic subunit type 2 beta
	<i>Dennd1b</i> ^e	DENN/MADD domain containing 1B
<i>Canq6</i>	<i>C1galt1</i> ^{a,b,c,d}	core 1 synthase, glycoprotein-N-acetylgalactosamine 3-beta-galactosyltransferase, 1
	<i>Hmox1</i> ^{b,c,d}	heme oxygenase 1
	<i>Apela</i> ^{b,c,d}	apelin receptor early endogenous ligand
	<i>Lpar2</i> ^{b,c,d,e}	lysophosphatidic acid receptor 2
	<i>Fkbp8</i> ^{b,d}	FK506 binding protein 8
	<i>Rab3a</i> ^{b,d,e}	RAB3A, member RAS oncogene family
	<i>Plvap</i> ^{b,d}	plasmalemma vesicle associated protein
	<i>Fcho1</i> ^e	FCH domain only 1
	<i>Rab8a</i> ^e	RAB8A, member RAS oncogene family
	<i>Ap1m1</i> ^e	adaptor-related protein complex AP-1, mu subunit 1
	<i>Klf2</i> ^{b,c,d}	kruppel-like factor 2
	<i>Canq7</i>	<i>Cav1</i> ^{b,c,d,e}
<i>Wnt2</i> ^{b,c,d}		wingless-type MMTV integration site family, member 2
<i>Canq8</i>	<i>Pik3ca</i> ^{b,d}	phosphatidylinositol-4,5-bisphosphate 3-kinase catalytic subunit alpha
<i>Canq9</i>	<i>Rab31</i> ^e	RAB31, member RAS oncogene family
	<i>Twsg1</i> ^{c,d}	twisted gastrulation BMP signaling modulator 1
	<i>Washc1</i> ^e	WASH complex subunit 1
	<i>Rab12</i> ^e	RAB12, member RAS oncogene family
	<i>Ptprm</i> ^d	protein tyrosine phosphatase, receptor type, M
	<i>Lama1</i> ^{c,d}	laminin, alpha 1
	<i>Ehd3</i> ^e	EH-domain containing 3
	<i>Ltbp1</i> ^{c,d}	latent transforming growth factor beta binding protein 1
	<i>Crim1</i> ^{c,d}	cysteine rich transmembrane BMP regulator 1
	<i>Cyp1b1</i> ^{b,c,d}	cytochrome P450, family 1, subfamily b, polypeptide 1
<i>Canq10</i>	<i>Vegfd</i> ^{b,c,d}	vascular endothelial growth factor D
	<i>Rab9</i> ^{d,e}	RAB9, member RAS oncogene family

Genes are listed under each locus in order of position (-10 -to- +10Mb, respectively). ^e, The association with endocytic vesicles arises as a criteria for inclusion in the table based on the known role of the endocytic protein, *Rabep2*, in collaterogenesis in certain classical strains of mice.^{22,25,26 in manuscript} ^f, See In Silico Analysis in Supplement for references linking *Cxcr4* to collaterogenesis.

Supplemental table IV. Coding and nonsense variants present in human orthologs of mouse genes known to (“Known genes”) and “Candidate genes” predicted to impair collaterogenesis. Single nucleotide variants (SNVs) obtained from the Genome Aggregation Database (gnomAD v3.1.2) are listed with their physical position on the indicated chromosome (Chr), rs number, amino acid substitution, and overall frequency of occurrence (Freq; see gnomAD for ancestry-specific frequencies). SNVs are listed if present in at least 10 individuals (Counts) out of the total Number of individuals genotyped and if predicted to be “probably damaging” by at least one of—and “possibly damaging” by at least one of: Polyphen2 (PP), SIFT or MetaLR (Meta) *in silico* algorithms per Ensemble (v109, 2/2023). Values calculated by Mutation Assessor (MutA), Revel and CADD prediction algorithms are also listed. If Polyphen2 values were not available, values for another algorithm were substituted for PP’s criterion (eg, see *RGS1*). **Red font**, probably damaging; **orange**, possibly damaging; **green**, tolerated; **blue**, uncertain. AA, African/African American; AJ, Ashkenazi Jewish; AM, Amish; EA, East Asian; FN, Finnish; LT, Latino/Admixed American; ME, Middle Eastern; SA, South Asian. Positions of residues of stops gained are given. Superscripted numbers attached to each “Known Gene” refer to the references given below the table that identified the gene using QTL analysis and CRISPR (*Rabep2*)¹ or reverse-genetic approaches (gene targeting, etc) for other genes.²⁻⁸ “Candidate Genes” are from Table 1.

Position	rs number	Coding SNV	Count	Number	Freq	PP	SIFT	Meta	MutA	Revel	CADD	Ancestry counts
Known Genes												
<i>RABEP2</i>¹ Chr 16												
28905025	rs527458355	p.Arg543His	24	152166	1.58e-4	0.994	0.00	0.673	0.763	0.647	28	23 AA, 1 SA
28905481	rs200118396	p.Arg508Ser	94	152154	6.18e-4	0.986	0.00	0.230	0.700	0.267	25	57 EU, 18 LT, 7 SA
28905727	rs184144701	p.Arg490Trp	12	152098	7.89e-5	0.997	0.00	0.216	0.781	0.367	29	8 EA, 3 AA, 1 AM
28906121	rs750752217	p.Arg441Cys	12	152182	7.89e-5	0.997	0.00	0.255	0.685	0.412	25	8 EU, 2 AA, 2 AJ
28911143	rs373485868	p.Arg311Cys	13	152178	8.54e-5	0.769	0.00	0.128	0.338	0.209	24	12 AA, 1 LT
28914373	rs200278634	p.Arg253Cys	14	152192	9.20e-5	0.825	0.03	0.164	0.314	0.138	24	11 AA, 3 EU
28914519	rs769480150	p.Ser204Leu	49	152196	3.22e-4	0.978	0.01	0.209	0.280	0.099	25	44 FN, 5 EU
<i>VEGFA</i>^{2,3} Chr 6												
43770809	rs1055085365	p.Glu35Ter	16	152154	1.05e-4	Stop gained		35/395				14 AA, 1, EU, 1 other
43770920	rs1004481569	p.Gly72Trp	11	152180	7.23e-5	0.984	0.000	0.061	-----	0.125	25	11 EU
<i>KDR</i>³ Chr 4												
55080075	rs151242590	p.Asp1313Asn	10	152224	6.57e-5	0.984	0.000	0.556	-----	0.000	24	5 AA, 4 EU, 1 other
55088923	rs373562441	p.Thr1152Met	33	152168	2.17e-4	0.898	0.010	0.816	0.697	0.000	28	32 AA, 1 LT
55088939	rs121917766	p.Pro1147Ser	12	152164	7.89e-5	0.998	0.010	0.847	0.536	0.000	26	8 EU, 3 AA, 1 LT
55089802	rs56302315	p.Ala1065Thr	62	152106	4.08e-4	0.955	0.010	0.663	0.089	0.000	32	42 AJ, 19 EU, 1 AA
55094936	rs140041720	p.Arg946His	37	152144	2.43e-4	0.980	0.020	0.464	0.153	0.000	28	17 EA, 8 AA, 7 LT, 5 EU
55097760	rs140761530	p.Pro839Leu	12	151660	7.91e-5	1.000	0.020	0.993	0.038	0.000	24	6 AA, 6 EA
55098158	rs145905001	p.Pro830Ser	11	152102	7.23e-5	1.000	0.010	0.792	0.560	0.000	26	6 EU, 4 LT, 1 AA
55098263	rs564385300	p.Gly795Arg	13	152160	8.54e-5	1.000	0.998	0.523	0.570	0.000	26	8 SA, 4 ME, 1 other
55114137	rs587778429	p.Pro263Thr	10	152068	6.58e-5	0.936	0.000	0.270	0.942	0.000	24	9 FN, 1 EU
<i>ADAMI7</i>³ Chr 2												
No predicted deleterious SNVs												
<i>DLA4</i>⁴ Chr 15												
40931580	rs145914797	p.Asp158Asn	19	152220	1.25e-4	0.326	0.030	0.871	0.769	0.000	26	19 AA
40936273	rs370339149	p.Arg429His	12	152220	7.88e-5	0.723	0.020	0.196	0.418	0.000	27	9 AA, 3 EU
40936539	rs201981567	p.Glu518Lys	33	152244	2.17e-4	0.986	0.010	0.826	0.912	0.000	28	20 FN, 9 EU, 2 AJ, 1 AA
40936645	rs375688749	p.Arg553Gln	13	152218	8.54e-5	0.992	0.060	0.775	0.615	0.000	26	9 EU, 2 FN, 1 AA, 1 SA
<i>NOTCH1</i>^{3,4} Chr 9												
136502059	rs201779159	p.Leu1805Pro	15	152080	9.86e-5	0.937	0.010	0.676	0.869	0.648	27	12 EU, 1 AA, 1 LT, 1 SA
136502383	rs373841359	p.Arg1758His	16	152240	1.05e-4	0.937	0.000	0.651	0.886	0.546	27	9 LT, 5 EU, 1 AA
136504793	rs375018022	p.Arg1633His	88	152208	5.78e-4	0.860	0.010	0.517	0.454	0.425	24	81 AA, 5 LT, 1 EU, 1 SA
136504896	rs543770603	p.Val1599Met	11	152200	7.23e-5	0.706	0.000	0.679	0.446	0.430	23	5 LT, 3 EU, 3 AA
136505359	rs765844768	p.Gly1513Ser	15	152216	9.85e-5	0.343	0.010	0.659	0.605	0.503	24	11 AA, 2, EU, 2 LT
136506571	rs149057410	p.Val1324Met	67	152154	4.40e-4	0.992	0.020	0.704	0.161	0.543	23	61 AA, 2 LT, 1 EU, 1 SA
136509030	rs201163739	p.Ser1004Leu	24	152260	1.58e-4	Stop gained		1004/2555			19	EU, 3 AJ, 2 LT
136509839	rs370797169	p.Arg955Cys	15	152238	9.85e-5	0.891	0.000	0.690	0.813	0.474	28	11 EU, 2 EA, 1 AA, 1 ME
136510659	rs201620358	p.Arg912Trp	333	152244	2.19e-3	0.846	0.000	0.573	0.239	0.402	25	235EU, 45LT, 25AA, 17 FN
136510719	rs578228721	p.Arg892Cys	46	152244	3.02e-4	0.952	0.000	0.778	0.621	0.715	24	40 LT, 4 AA, 1 EU, 1 other

136511244	rs559917218	p.Pro832Leu	56	152138	3.68e-4	0.999	0.010	0.757	0.603	0.680	28	47 LT, 5 AA, 3 EU, 1 other
136513054	rs201620755	p.Gly812Arg	39	151732	2.57e-4	1.000	0.030	0.743	0.443	0.724	25	36 AA, 3 EU
136513129	rs199672693	p.Asn787Asp	16	152062	1.05e-4	0.999	0.010	0.802	0.578	0.616	27	13 LT, 1 AA, 2 other
136514511	rs201662530	p.Gly736Arg	20	152234	1.31e-4	0.189	0.010	0.626	0.657	0.696	13	12 AA, 7 EU, 1 LT
136517898	rs200562991	p.Thr432Met	19	152072	1.25e-4	1.000	0.000	0.891	0.503	0.835	26	6 EU, 5 AJ, 4 SA, 3LT, 1 EA
136519457	rs376104770	p.Pro284Leu	19	152244	1.25e-4	0.910	0.180	0.877	0.448	0.743	23	14 EU, 5 LT
136519469	rs367825691	p.Asn280Ser	24	152172	1.58e-4	0.999	0.040	0.601	0.037	0.517	24	20 EU, 3 LT, 1 AA
136522891	rs150737112	p.Arg234His	63	152172	4.14e-4	0.952	0.600	0.515	0.100	0.462	23	32 EU, 24 LT, 6 AA, 1 SA
136522918	rs553542677	p.Ser225Trp	10	152228	6.57e-5	0.999	0.010	0.744	0.461	0.736	29	10 AA
136523138	rs750242131	p.Gly152Ser	22	152222	1.45e-4	0.742	0.020	0.909	0.809	0.788	24	14 AA, 8 EU

ADAM10³ Chr 15

No predicted deleterious SNVs

EPHA4⁵ Chr 2

221426033	rs141387215	p.Val986Ile	93	151988	6.12e-4	0.994	0.000	0.514	0.692	0.328	26	87 AA, 5, LT, 1 EU
221436595	rs370645355	p.Arg717Ile	17	152210	1.12e-4	0.942	0.000	0.526	0.501	0.577	26	15 EU, 1 AA, 1 LT

CLIC4^{6,7} Chr 1

No predicted deleterious SNVs

GJA4⁸ Chr 1

34794466	rs373204338	p.Val85Ile	18	152108	1.18e-4	0.992	0.000	0.973	0.543	0.784	27	13 SA, 5 EU
34794745	rs138853660	p.Gly178Ser	12	152164	7.89e-5	0.999	0.000	0.957	0.833	0.952	28	12 EU
34794836	rs147387551	p.Ile208Thr	42	152092	2.76e-4	0.462	0.000	0.917	0.948	0.934	27	36 EU, 6 AA
34794925	rs201475159	p.Arg238Trp	10	152148	6.57e-5	0.167	0.010	0.847	0.314	0.313	21	7 AA, 3 EA
34795178	rs151235389	p.Arg322His	10	151836	6.59e-5	0.837	0.010	0.852	0.560	0.339	23	5 AA, 2 FN, 2 LT, 1 EU

Candidate Genes

SOX13 Chr 1

204116516	rs1284301034	p.Glu143Gly	10	152222	6.57e-5	0.994	0.00	0.965	0.773	0.847	30	10 LT
204122265	rs756405105	p.Ala297Asp	11	152150	7.23e-5	0.976	0.01	0.967	0.866	0.696	25	10 F, 1 EU
204122282	rs199517579	p.Glu303Lys	41	151944	2.70e-4	0.665	0.01	0.922	0.853	0.482	26	28 Lat, 11 EU, 2 AA
204122959	rs201772428	p.Arg377His	150	152180	9.86e-4	0.996	0.00	0.944	0.832	0.495	24	111 EU, 12 AA, 10 F, 10 SA
204123205	rs561040843	p.Asp410Tyr	12	152242	7.88e-5	0.678	0.00	0.930	0.835	0.760	33	11 SA, 1 EA
204123685	rs771489813	p.Arg419Gln	23	152140	1.51e-4	0.992	0.01	0.954	0.875	0.643	32	23 AA

CYB5R1 Chr 1

202963091	rs368686887	p.Trp240Cys	17	152154	1.12e-4	1.000	0.00	0.849	0.959	0.860	31	16 EA, 1 SA [stop gained 240/305]
202964651	rs2232845	p.Arg174Ter	12	152174	7.89e-5	Stop gained 174/305					31	10 AA, 2 F
202966750	rs199636712	p.Thr55Met	13	152178	8.54e-5	0.877	0.00	0.762	0.899	0.502	33	13 LT

RGS1 Chr 1

192579159	rs150745219	p.Arg156Gln	31	151926	2.04e-4	-----	0.000	0.288	0.821	0.391	31	20 EU, 8 AA
-----------	-------------	-------------	----	--------	---------	-------	-------	-------	-------	-------	----	-------------

ASPM Chr 1

197089983	rs542967760	p.Pro3311Ala	11	151616	7.26e-5	0.001	0.650	0.321	0.731	0.459	27	11 LT
197090384	rs368682161	p.Leu3214Ser	13	152022	8.55e-5	0.999	0.020	0.164	0.795	0.371	28	9 EU, 2 LT, 1 AA
197090909	rs140679756	p.Arg3193Cys	14	151970	9.21e-5	1.000	0.030	0.714	0.848	0.585	26	7 AA, 7 EU
197090947	rs193251130	p.Gln3180Pro	199	152122	1.31e-3	0.890	0.010	0.287	0.735	0.282	21	184 SA, 5 AA, 5 EU, 3 LT
197091912	rs150906798	p.Ile3147Val	12	152018	7.89e-5	0.968	0.050	0.437	0.474	0.097	23	11 EU, 1 LT
197091956	rs36004306	p.Leu3132Pro	14	152004	9.21e-5	0.924	0.000	0.355	0.338	0.336	22	12 EU, 1 SA, 1 LT
197093059	rs146444278	p.Arg3096Gln	13	151868	8.56e-5	0.998	0.010	0.446	0.739	0.477	25	7 EU, 6 AA
197093074	rs147005963	p.Arg3091His	85	151900	5.60e-4	0.997	0.000	0.560	0.739	0.668	23	81 AA, 2 EU, 2 LT
197094116	rs753961004	p.Lys3018Glu	10	151856	6.59e-5	0.643	0.010	0.684	0.322	0.415	25	10 AA
197096010	rs149690383	p.Leu2992Pro	39	151868	2.57e-4	0.950	0.110	0.753	0.158	0.419	11	33 EU, 4 AA, 1 FN, 1 LT
197096099	rs533985055	p.Gln2962His	15	151850	9.88e-5	1.000	0.000	0.846	0.964	0.764	24	15 AA
197100727	rs112946633	p.Arg2842Trp	13	151754	8.57e-5	0.833	0.000	0.417	0.766	0.370	22	12 AA, 1 LT
197101048	rs372416792	p.Phe2735Val	71	151798	4.68e-4	0.875	0.020	0.462	0.838	0.303	17	69 SA, 2 AA
197101970	rs752506858	p.Phe2427Leu	25	151764	1.65e-4	0.948	0.020	0.537	0.645	0.498	26	17 FN, 8 EU
197102137	rs190693455	p.Arg2372Gly	48	151816	3.16e-4	0.778	0.020	0.288	0.673	0.294	19	42 EA
197102145	rs372076208	p.Gln2369Pro	14	151786	9.22e-5	0.830	0.000	0.426	0.330	0.354	18	14 AA

197102158	rs371212366	p.Gln2365Glu	15	151670	9.89e-5	0.990	0.000	0.732	0.905	0.489	24	15 AA
197102400	rs371321801	p.Ser2284Phe	18	151778	1.19e-4	0.945	0.000	0.475	0.887	0.260	22	17 AA, 1 EU
197102455	rs200800956	p.Ala2266Thr	13	151698	8.57e-5	0.999	0.000	0.718	0.944	0.462	23	8 EU, 2 AJ, 1 SA, 1 EA
197103304	rs141715950	p.Met1983Leu	175	151904	1.15e-3	0.933	0.000	0.234	0.956	0.235	23	131 EU, 15 AA, 15 LT
197103354	rs140834556	p.Gln1966Pro	19	151932	1.25e-4	0.712	0.010	0.367	0.772	0.299	14	13 EU, 6 AA
197103467	rs554548758	p.Gln1928His	12	151888	7.90e-5	0.999	0.000	0.714	0.935	0.581	20	9 SA, 1 EU, 1 AA
197103667	rs527602809	p.Lys1862Glu	37	151950	2.44e-4	0.861	0.020	0.490	0.893	0.292	22	18 LT, 16 SA
197103741	rs144969324	p.Asn1839Ser	29	151844	6.58e-6	0.973	0.030	0.677	0.972	0.592	24	25 EA, 1 SA, 3 LT
197103799	rs41299625	p.Arg1818Cys	156	151900	1.03e-3	0.998	0.000	0.617	0.988	0.538	25	122 EU, 14 AA, 2 SA, 1 EA
197104113	rs141297873	p.Arg1713His	12	151814	7.90e-5	0.965	0.010	0.589	0.907	0.586	19	6 LT, 3 EU, 2 ME, 1 AA
197104114	rs143911853	p.Arg1713Cys	16	151852	1.05e-4	0.995	0.020	0.619	0.854	0.626	24	10 AA, 5 EU, 1 EA
197104266	rs147839989	p.Ile1662Ser	16	151894	1.05e-4	0.999	0.000	0.770	0.973	0.838	26	13 EU, 2 LT
197104276	rs560847421	p.Val1659Phe	14	151830	9.22e-5	0.959	0.000	0.523	0.909	0.390	17	14 EA
197104709	rs375778017	p.Ile1514Met	12	151928	7.90e-5	0.944	0.010	0.434	0.808	0.321	17	12 AA
197104755	rs140119882	p.Arg1499Leu	68	151794	4.48e-4	0.999	0.000	0.858	0.957	0.740	26	66 AA, 2 LT
197104849	rs189918817	p.Ala1468Thr	25	151870	1.65e-4	1.000	0.010	0.684	0.906	0.483	24	18 EU, 4 AA, 2 LT, 1 FN
197105035	rs145662604	p.Ala1406Thr	36	151804	2.37e-4	1.000	0.040	0.217	0.926	0.0284	24	36 AA
197105077	rs762353508	p.Arg1392Ter	10	151786	6.59e-5	Stop gained		1392/3477				7 LAT, 2 FN, EA
197105103	rs375240502	p.Met1383Thr	16	151948	1.05e-4	0.970	0.20	0.248	0.499	0.305	24	14 AA, 2 LT
197105116	rs768625023	p.Ser1379Pro	14	151950	9.21e-5	0.980	0.000	0.425	0.938	0.457	25	14 AA
197117899	rs376541100	p.Ala1319Ser	11	152060	7.23e-5	0.703	0.000	0.649	0.935	0.282	20	5 EA, 2 EU, 1 LT, 1 SA, 1AJ
197122013	rs142214506	p.Ala1258Thr	42	151896	2.77e-4	0.494	0.020	0.469	0.657	0.346	24	42 AA
197133493	rs375901171	p.Arg759Gln	16	152094	1.05e-4	0.981	0.000	0.388	0.467	0.375	25	12 EA, 4 EU
197133494	rs777867809	p.Arg759Trp	90	152112	5.92e-4	0.997	0.000	0.365	0.467	0.366	27	88 LT, 2 AA
197139844	rs112997359	p.Ser650Cys	26	152160	1.71e-4	0.538	0.010	0.150	0.518	0.019	16	26 AA
197142535	rs144049904	p.Arg573Trp	317	152070	2.08e-3	0.613	0.000	0.302	0.560	0.115	22	176 EU, 107LT, 15AA, 7AJ

CFHRI Chr 1. No predicted damaging variants

CFHRA Chr 1

196902480	rs199547603	p.Arg41Ter	122	151486	8.05e-4	Stop gained		41/578				118 AA, 3 LT, 1 SA
196902563	rs201480125	p.Trp68Ter	65	151082	4.30e-4	Stop gained		68/578				54 AA, 5 EU, 3 LT
196907017	rs199731883	p.Ser199Tyr	31	151196	2.05e-4	0.989	0.000	0.501	0.915	0.250	17	31 AA
196907017	rs199731883	p.Ser199Phe	16	151196	1.06e-4	0.989	0.000	0.501	0.905	0.250	17	8 EU, 7 AJ, 1 LT
196907468	rs183705632	p.Gly257Arg	373	150964	2.47e-3	0.632	0.000	0.426	0.946	0.292	19	347 EU, 22 FN, 3 AJ
196912826	rs77776928	p.Tyr362His	241	151618	1.59e-3	0.970	0.010	0.354	0.971	0.234	21	223 AA, 11 LT, 2 EU, 1 ME
196914648	rs376896638	p.Trp445Ter	45	150272	2.99e-4	Stop gained		445/578				41 SA, 3 AA
196915062	rs575550227	p.Gln488His	19	151572	1.25e-4	0.749	0.010	0.249	0.522	0.190	14	17 AA, 2 LT
196915069	rs373767199	p.Tyr491Asp	12	151644	7.91e-5	0.968	0.000	0.684	0.989	0.482	21	11 AA, 1 LT
196918321	rs201727614	p.Lys551Thr	54	151532	3.56e-4	0.600	0.020	0.462	0.645	0.361	14	37 EU, 13 AA, 4 FN

JAK3 Chr 19

17826901	rs200580168	p.Leu1073Phe	50	152210	3.28e-4	0.946	0.000	0.372	0.251	0.478	25	29 EU, 18 FN
17832539	rs148688786	p.Arg887His	15	152218	9.85e-5	0.956	0.060	0.611	0.103	0.511	25	5 EU, 3 SA, 3 AJ, 2 EA
17832681	rs200077579	p.Arg840Cys	36	152208	2.37e-4	0.863	0.000	0.681	0.477	0.581	25	12 EU, 11 AM, 8 LT, 2 SA
17834630	rs149982493	p.Pro764Leu	15	150934	9.94e-5	0.619	0.000	0.535	0.908	0.387	25	14 AA, 1 EU
17841389	rs373046546	p.Thr381Asn	17	152188	1.12e-4	0.586	0.010	0.366	0.775	0.311	25	17 AA
17842528	rs202167678	p.Val217Met	16	152258	1.05e-4	0.905	0.020	0.456	0.694	0.362	22	14 AJ, 2 EU
17843115	rs149579831	p.Gly160Cys	15	152204	9.86e-5	0.508	0.000	0.403	0.574	0.360	26	13 EU, 1 LT
17844395	rs145500023	p.Thr8Met	83	152162	5.45e-4	0.973	0.060	0.518	0.179	0.293	22	63 EU, 10 AA, 8 LT, 1 FN

YJEFN3 Chr19

19532678	rs61749571)	p.Gly88Glu	122	152208	1.84e-4	0.926	0.010	0.148	0.590	0.293	28	114 AA, 4 LT, 3 EU, 1 SA
19535408	rs141151340	p.Cys167Trp	14	152190	9.20e-5	0.906	0.010	0.251	0.831	0.426	15	9 EA, 3 SA, 1 EU, 1 LT
19535632	rs146733860	p.Thr216Arg	804	152200	5.28e-3	0.991	0.000	0.146	0.480	0.289	23	619 EU, 72 AA, 53FN, 38LT
19535658	rs200227282	p.Val225Met	231	152192	1.52e-3	0.960	0.000	0.281	0.882	0.263	26	222 AA, 6 LT, 1 EA
19537411	rs545964787	p.Phe263Leu	12	152212	7.88e-5	0.971	0.010	0.200	0.612	0.211	24	9 SA, 1 EU, 1 AA
19537487	rs1162772387	p.Pro288Leu	24	152246	1.58e-4	0.998	0.000	0.267	0.803	0.415	28	24 EU

CILP2 Chr 19

19540306	rs201714553	p.Val89Gly	68	152154	4.47e-4	0.742	0.000	0.154	0.927	0.000	27	62 FN, 6 EU
----------	-------------	------------	----	--------	---------	-------	-------	-------	-------	-------	----	-------------

19540374	rs200679414	p.Arg112Cys	316	152208	2.08e-3	0.958	0.040	0.092	0.709	0.000	26	185FN, 108EU, 12AA, 4LT
19542944	rs146789008	p.Gly317Arg	16	152192	1.05e-4	1.000	0.000	0.512	0.980	0.000	12	16 EU
19544001	rs146322371	p.Glu486Lys	42	152228	2.76e-4	0.984	0.000	0.245	0.828	0.000	24	37 AA, 3 EU, 2 LT
19544086	rs139539877	p.Pro514Leu	40	152266	2.63e-4	0.804	0.000	0.287	0.772	0.000	20	31 EU, 4 AA, 3 LT, 1 ME
19544610	rs758468698	p.Gly689Ser	10	152182	6.57e-5	1.000	0.010	0.321	0.809	0.000	27	10 EU
19544925	rs532951417	p.Pro794Ser	14	152214	9.20e-5	0.991	0.000	0.078	0.508	0.000	23	14 SA

DI3RIK Not annotated in human

BABAMI Chr 19

17268634	rs774465344	p.Leu2Phe	73	152012	4.80e-4	In non-can. transcript; uncertain tests					56 EU, 8 LT, 7 AA	
17268640	rs182898955	p.Arg4Ser	239	152040	1.57e-3	In non-can. transcript; uncertain tests					235 AA, 3 LT, 1 EU	
17268756	rs138467832	p.Gly13Arg	11	152114	7.23e-5	In non-can. transcript; 0.098 PP					11 EA	
17271654	rs115366940	p.Gly115Ser	499	152204	3.28e-3	0.812	0.010	0.237	0.657	0.000	18	457 AA, 21 LT, 13 EU, 1 SE
17276515	rs374131612	p.Pro197Leu	16	152154	1.05e-4	1.000	0.000	0.346	0.802	0.000	26	7 EU, 6 AA, 2 LT
17276536	rs550805861	p.Thr204Met	50	152194	3.29e-4	0.967	0.000	0.116	0.707	0.000	22	47 SA, 2, EU, 1 EA
17276581	rs200016717	p.Arg219His	52	152196	3.42e-4	0.999	0.000	0.315	0.818	0.000	32	26 EU, 19 AZ, 4 AA, 2 LT

ZFP709 Not annotated in human

OLFR374 Not annotated in human

ZFP372 Not annotated in human

CAV2 Chr 7

116499905	rs374156174	p.Pro42Ser	11	152078	7.23e-5	0.900	0.000	0.907	0.875	0.828	27	11 EU
116500365	rs149320804	p.Lys86Glu	19	152192	1.25e-4	0.965	0.000	0.897	0.848	0.819	28	9 AJ, 5 LT, 4 EU

IQUB Chr 7

123452867	rs146017906	p.Tyr751Cys	11	152068	7.23e-5	----	0.000	0.219	0.873	0.500	28	6 AA, 2 EA, 3 SA, 1 EU
123457529	rs145461420	p.Ala682Val	374	151988	2.46e-3	----	0.050	0.094	0.837	0.110	24	286 EU, 58 AA, 19 LT, 4 FN
123461451	rs60409072	p.Arg638Gln	480	151774	3.16e-3	----	0.010	0.208	0.887	0.317	26	457 AA, 14 LT, 2 EU, 1 ME
123461494	rs373146060	p.Arg624Trp	17	151688	1.12e-4	----	0.010	0.142	0.657	0.153	22	12 SA, 2 EU, 1 AA, 1 EA
123464949	rs1431266872	p.Met548Val	24	151880	1.58e-4	----	0.010	0.142	0.697	0.120	22	24 LT
123464949	rs199522362	p.Leu547Phe	88	151726	5.80e-4	----	0.020	0.511	0.869	0.528	26	31 AJ, 25 LT, 20 EU, 6 AA
123469222	rs74488511	p.Thr525Ala	16	152114	1.05e-4	----	0.010	0.234	0.649	0.328	25	16 EA
123469294	rs149316783	p.Ile501Phe	36	152194	2.37e-4	----	0.000	0.327	0.847	0.473	24	34 AA, 1 LT
123479859	rs144590492	p.Gly449Val	11	151998	7.24e-5	----	0.000	0.296	0.808	0.332	24	10 AA, 1 LT
123479868	rs148490443	p.Ala446Val	52	152062	3.42e-4	----	0.000	0.318	0.818	0.248	26	39 EU, 5 LT, 4 FN, 2 AA
123479896	rs143618132	p.Leu437Phe	30	152044	1.97e-4	----	0.000	0.448	0.864	0.498	24	26 EU, 2 LT, 1 AA
123479960	rs201714151	p.Gln415His	10	152136	6.57e-5	----	0.010	0.138	0.750	0.132	23	10 LT
123496858	rs370004563	p.Val358Ile	19	152006	1.25e-4	----	0.010	0.256	0.760	0.011	22	19 AA
123502618	rs201786274	p.Tyr334Ter	15	152130	9.86e-5	Stop gained 334/791					13 AJ, 2 EU	
123502948	rs760765844	p.Thr288Met	15	151946	9.87e-5	----	0.000	0.467	0.921	0.481	25	4 EU, 4 AA, 2 LT, 2FN, 2EA
123503030	rs372053513	p.Thr261Ala	13	152202	8.54e-5	----	0.000	0.377	0.849	0.439	25	6 AJ, 4 LT, 1 AA, 1 SA
123512135	rs140652989	p.Ser69Ter	15	152164	9.86e-5	Stop gained 69/791					11 EU, 2 AM, 1 AA, 1 FN	

PLDI Chr 3

171603170	rs140343065	p.Val1045Met	19	152140	1.25e-4	0.999	0.000	0.186	0.955	0.371	27	18 AA, 1 LT
171612393	rs567323716	p.Arg923His	14	152182	9.20e-5	0.994	0.000	0.398	0.557	0.435	27	11 SA, 3 EA
171620433	rs191205035	p.Tyr894Ser	65	152124	4.27e-4	0.981	0.000	0.275	0.957	0.557	31	42 LT, 18 EU, 3 AA
171644913	rs143219477	p.Tyr847Cys	30	152206	1.97e-4	0.988	0.000	0.263	0.964	0.449	27	29 AA, 1 LT
171644953	rs142188788	p.Gly834Ser	12	152156	7.89e-5	0.999	0.000	0.177	0.443	0.138	25	8 AA, 4 EU
171659247	rs540439098	p.Asp799Asn	10	152216	6.57e-5	0.969	0.000	0.210	0.908	0.308	25	8 AA, 1 EU, 1 LT
171659251	rs140049612	p.Ile797Met	19	152284	1.25e-4	0.938	0.000	0.388	0.965	0.372	16	17 EU, 2 AA
171662164	rs745485055	p.Arg746Cys	11	152120	7.23e-5	0.956	0.000	0.269	0.934	0.625	32	7 LT, 3 EU, 1 AA
171676758	rs146885315	p.Arg691Leu	52	152224	3.42e-4	0.972	0.000	0.225	0.652	0.584	27	45 EU, 7 FN
171676764	rs139363214	p.Ala689Val	10	152198	6.57e-5	0.972	0.000	0.166	0.570	0.276	27	8 EU, 1 SA, 1 LT
171676807	rs202167212	p.Arg675Trp	11	152202	7.23e-5	0.999	0.000	0.181	0.729	0.420	32	8 LT, 2 EU, 1 FN
171688711	rs80085541	p.Arg502Trp	26	152106	1.71e-4	0.930	0.000	0.189	0.638	0.236	29	17 EU, 5 EA, 2 AA
171688812	rs374719323	p.Val468Asp	13	152188	8.54e-5	0.938	0.000	0.462	0.978	0.632	27	6 EU, 6 LT
171688863	rs141086000	p.Pro451Leu	10	152082	6.58e-5	0.996	0.000	0.294	0.958	0.597	26	9 EU, 1 AA
171699746	rs201602698	p.Ala409Gly	12	152214	7.88e-5	0.999	0.000	0.507	0.892	0.592	33	9 EU, 1 AA, 1 FN
171709672	rs371154750	p.Arg317Trp	11	152112	7.23e-5	0.666	0.000	0.590	0.768	0.740	29	6 EU, 2 AA, 2 SA, 1 ME

171713981	rs370939132	p.Val275Ile	14	152110	9.20e-5	0.900	0.000	0.468	0.735	0.230	25	9 EA, 4 EU
171724745	rs149535568	p.Gly237Cys	139	152200	9.13e-4	0.985	0.000	0.932	0.609	0.809	24	116 EU, 23 AA
171724759	rs147193827	p.Gly232Glu	13	152174	8.54e-5	0.872	0.000	0.929	0.837	0.870	25	13 EA
FAT4 Chr 4												
125316596	rs201009019	p.Gly62Ala	103	152170	6.77e-4	0.991	0.010	0.753	0.446	0.711	28	79 EU, 10 AA, 9 SA, 2 LT
125318238	rs370300509	p.Asp609Glu	40	152182	2.63e-4	0.167	0.000	0.404	0.972	0.475	15	37 AA, 2 LT, 1 EU
125319589	rs200529379	p.Arg1060Cys	10	152120	6.57e-5	0.990	0.000	0.402	0.630	0.474	26	6 FN, 4 EU
125319916	rs190175933	p.Arg1169Trp	16	152096	1.05e-4	0.594	0.000	0.404	0.446	0.467	25	7 EU, 7 AA, 1 FN, 1 LT
125320411	rs368607709	p.Val1334Met	19	152100	1.25e-4	0.995	0.000	0.449	0.825	0.349	26	10 AA, 7 EU, 1 EA
125320580	rs201934636	p.Ile1390Thr	24	152224	1.58e-4	0.127	0.000	0.188	0.946	0.384	25	20 EU, 4 AA
125320694	rs772537061	p.Ser1428Phe	16	152206	1.05e-4	0.969	0.020	0.024	0.382	0.360	25	16 LT
125406973	rs201887525	p.Arg1801Trp	20	152004	1.32e-4	0.998	0.000	0.019	0.391	0.289	23	15 EU, 3 EA, 1 SA, 1 AA
125408666	rs139716832	p.Tyr1931Cys	90	152066	5.92e-4	0.994	0.010	0.024	0.603	0.518	27	74 EU, 10 AA, 4 Lt, 1 FN
125408675	rs200026034	p.Ile1934Thr	13	152118	8.55e-5	0.892	0.000	0.330	0.763	0.338	25	13 AA
125416574	rs559079176	p.Arg2324Trp	22	152062	1.45e-4	0.594	0.000	0.029	0.923	0.409	22	19 LT, 1 EU, 1 SA
125434305	rs534302520	p.Asn2360Ser	26	152186	1.71e-4	0.992	0.000	0.526	0.841	0.441	25	16 AA, 7 LT, 2EU
125446357	rs139924242	p.Ser2422Cys	16	152106	1.05e-4	0.980	0.000	0.316	0.538	0.390	27	16 AA
125446405	rs376545643	p.Val2438Phe	12	152016	7.89e-5	0.926	0.010	0.232	0.154	0.296	24	9 EU, 2 AA
125449646	rs781160819	p.Tyr2879Cys	10	152160	6.57e-5	0.998	0.000	0.586	0.982	0.719	27	10 AA
125449741	rs148655455	p.Tyr2911His	25	152176	1.64e-4	0.104	0.000	0.583	0.976	0.727	26	25 EU
125450461	rs200702071	p.Ala3151Thr	41	152102	2.70e-4	0.594	0.020	0.014	0.127	0.198	24	23 SA, 8 EU, 5 LT, 2AA, 1AJ
125450974	rs181641041	p.Val3322Met	12	152208	7.88e-5	0.999	0.000	0.459	0.889	0.502	27	12 AA
125451346	rs756625118	p.Ile3446Val	10	152140	6.57e-5	0.511	0.040	0.325	0.772	0.290	24	10 EU
125451386	rs190233104	p.Pro3459Leu	11	152056	7.23e-5	0.226	0.000	0.204	0.718	0.342	23	5 SA, 5 EU 1 EA
125451653	rs79726583	p.Tyr3548Cys	23	152156	1.51e-4	0.924	0.010	0.498	0.940	0.335	27	23 AA
125452163	rs139635339	p.Arg3718His	19	152144	1.25e-4	0.987	0.040	0.303	0.508	0.303	25	13 EU, 4 AA, 1 Lt 1 SA
125452390	rs201859188	p.Arg3794Trp	28	152184	1.84e-4	0.990	0.000	0.432	0.486	0.626	24	14 LT, 8 EU, 4 AA, 1 FN
125452472	rs142857910	p.Arg3821Gln	11	152194	7.23e-5	0.942	0.010	0.370	0.091	0.387	23	9 AA, 1 LT, 1 SA
125468638	rs149250709	p.Ala4011Val	30	152060	1.97e-4	0.800	0.000	0.641	0.806	0.790	25	19 AA, 6 LT, 4 EU
125468676	rs138019311	p.Arg4024Trp	488	152088	3.21e-3	0.932	0.020	0.400	0.467	0.489	23	353EU,42AJ 33LT,10 other
125468691	rs140544054	p.Ala4029Thr	13	152094	8.55e-5	0.563	0.040	0.642	0.570	0.658	28	11 AJ, 2 EU
125477197	rs150804471	p.Ile4114Met	70	149916	4.67e-4	0.675	0.040	0.336	0.237	0.290	23	63 AA, 3 LT, 4 other
125481563	rs148170326	p.Arg4216His	61	152148	4.01e-4	0.725	0.030	0.344	0.490	0.404	23	54 EU, 3 AA, 2 LT, 1 FN
125490017	rs773916430	p.Arg4401Cys	10	151952	6.58e-5	0.809	0.000	0.579	0.821	0.582	25	8 AA, 2 EU
125491107	rs552252173	p.His4764Arg	12	152154	7.89e-5	0.978	0.000	0.208	0.179	0.141	15	11 AA, 1 LT
125491128	rs201633380	p.Arg4771His	31	152136	2.04e-4	0.994	0.000	0.546	0.179	0.286	27	28 LT, 2 AA, 1 EU
125491178	rs138173652	p.Gly4788Arg	14	152084	9.21e-5	0.896	0.000	0.811	0.202	0.619	24	6 LT, 6 EU, 1 AA, AJ
125491582	rs752311257	p.Lys4922Asn	10	152182	6.57e-5	0.058	0.000	0.333	0.615	0.106	11	8 FN, 2 EU
USP13 Chr 3												
179707000	rs141550831	p.Trp182Arg	41	152118	2.70e-4	-----	0.000	0.256	0.852	0.683	29	38 EU, 3 AA
179708886	rs200478981	p.Ala245Val	16	152082	1.05e-4	-----	0.000	0.552	0.996	0.591	25	15 EU, 1 LT
179740305	rs776225594	p.Pro438Leu	12	152094	7.89e-5	-----	0.010	0.537	0.508	0.534	25	11 EU, 1 AA
179742254	rs200761055	p.Arg480Cys	132	152190	8.67e-4	-----	0.010	0.283	0.933	0.414	27	51 SA, 34 LT, 39 EU, 2 AA
179754824	rs200079140	p.Arg672His	12	152140	7.89e-5	-----	0.000	0.207	0.909	0.368	32	5 EU, 4 AA, 2 EA, 1 SA
179765710	rs199954201	p.Asn754Ser	20	152262	1.12e-4	-----	0.000	0.153	0.856	0.385	27	17 EU, 3 AA
GMI527 Not annotated in human												
ARHGAP28 Chr 18												
6824836	rs188975691	p.Arg66His	28	152122	1.84e-4	0.989	0.040	0.221	0.603	0.000	27	18 EA, 5 AA, 1SA, 1EU, 1LT
6882201	rs186052265	p.His452Arg	14	152228	9.20e-5	0.362	0.010	0.085	0.790	0.165	24	11 Lt, 2 EU, 1 AA
6890539	rs74414891	p.Arg615Gln	74	152194	4.86e-4	0.980	0.020	0.092	0.826	0.179	25	71 AA, 3 LT
6890539	rs74414891	p.Arg615Leu	358	152190	2.35e-3	0.980	0.020	0.092	0.826	0.179	25	119SA, 94EU, 87EA, 18AA
6898484	rs756134118	p.Trp641Ter	15	151968	9.87e-5	Stop gained 641/670						15 AA
6912083	rs142653243	p.Ala707Ser	20	152118	1.31e-4	0.552	0.020	0.032	0.625	0.000	25	18 AA, 2 other
RMDN2 Chr 2												
37929288	rs1049449941	p.Ser4Tyr	21	152148	1.38e-4	0.839	0.000	0.232	0.799	0.111	23	21 AA
37929701	rs199499480	p.Ser142Gly	62	152238	4.07e-4	0.959	0.000	0.307	0.881	0.199	25	52 EU, 9 AA, 1 LT

37951261	rs140191801	p.Arg16Ter	391	151994	2.57e-3	Stop gained	16/573										360 AA, 4 EU, 3 ME
37951541	rs370260752	p.Asp109Gly	16	152096	1.05e-4	0.952	0.010	0.088	-----	0.041	17						15 EU, 1 other
37951915	rs78569430	p.Asp234Tyr	1078	151994	7.09e-3	0.711	0.000	0.079	-----	0.031	17						1005 AA, 40 LT, 12 SA
37974065	rs140735845	p.Glu160Ter	43	152150	2.83e-4	Stop gained	338/573										42 AA, 1 EU
37975239	rs143149132	p.Arg219Ter	10	152062	6.58e-5	Stop gained	397/573										8 EU, 1 AA, 1 LT
37997430	rs779349930	p.Ser320Arg	10	152110	6.57e-5	0.816	0.000	0.240	0.873	0.353	24						10 SA
38004146	rs147688126	p.Asp370Val	21	152168	1.38e-4	0.302	0.000	0.263	0.840	0.244	31						11 LT, 6 EU, 3 SA
MYOMI	Chr 18																
3067528	rs764839969	p.Gly1598Arg	19	152212	1.25e-4	-----	0.000	0.808	0.938	0.889	25						17 EU, 2 SA
3067534	rs375965840	p.Val1596Met	13	152176	9.20e-5	-----	0.000	0.666	0.816	0.558	25						11 SA 3 AA
3071887	rs373419422	p.Arg1571Cys	26	152142	1.71e-4	-----	0.010	0.324	0.879	0.568	33						20 AA, 5 LT, 1 EU
3083991	rs730880167	p.Ile1459Lys	61	152044	4.01e-4	-----	0.000	0.268	0.760	0.377	32						59 EU, 2 FN
3086046	rs190368385	p.Ile1415Val	29	152220	1.91e-4	-----	0.000	0.636	0.503	0.552	23						28 AA, 1 LT
3086108	rs374142554	p.Asp1394Gly	10	152218	6.57e-5	-----	0.000	0.532	0.696	0.664	32						9 LT, 1 AA
3086112	rs371239754	p.Lys1393Glu	50	152230	3.28e-4	-----	0.000	0.629	0.668	0.625	28						35 AA, 10 LT, 2 EU
3102501	rs147050513	p.Arg1183Gln	36	152094	2.37e-4	-----	0.000	0.711	0.850	0.517	24						19 AJ, 7 EU, 6 LT, 3 AA
3116411	rs371066861	p.Val1075Met	17	152172	1.12e-4	-----	0.000	0.439	0.807	0.519	24						7 EU, 6 AA, 3 LT
3119890	rs377512048	p.Glu1033Lys	24	152194	1.58e-4	Stop gained	1033/1685										23 AA, 1 LT
3119949	rs557671408	p.Ala1013Val	115	152152	7.56e-4	-----	0.000	0.617	0.973	0.808	29						111 SA, 1AA, 1 LT
3135618	rs18388166	p.Arg713His	11	152078	7.23e-5	-----	0.000	0.426	0.891	0.525	27						7 AA, 3 EU, 1 ME
3135619	rs375858580	p.Arg713Cys	14	151996	9.21e-5	-----	0.000	0.463	0.532	0.535	32						11 EU, 1 AA, 1 EA
3135624	rs548747720	p.Arg711His	12	152096	7.89e-5	-----	0.000	0.507	0.898	0.751	27						8 EU, 3 AA, 1 EA
3141941	rs200179081	p.Lys675Glu	44	152166	2.89e-4	-----	0.010	0.390	0.896	0.499	32						37 EU, 5 AA, 1 LT, 1 FN
3151801	rs185573271	p.Ser579Phe	45	152174	2.96e-4	-----	0.000	0.357	0.518	0.601	31						25 EU, 18 LT, 1 AA
3154963	rs370063864	p.Gly543Arg	22	152110	1.45e-4	-----	0.000	0.389	0.846	0.599	31						20 LT, 2 AA
3154984	rs367903122	p.Asp536Asn	13	152202	8.54e-5	-----	0.000	0.472	0.785	0.620	26						8 AJ, 4 AA, 1 EU
3164292	rs1278590083	p.Tyr496Cys	17	152234	1.12e-4	-----	0.000	0.624	0.851	0.697	29						17 LT
3164421	rs368424215	p.Ser453Ter	17	152248	6.57e-6	Stop gained	453/1685										17 AA
3174156	rs1435418077	p.Gly359Arg	14	152218	9.20e-5	-----	0.000	0.821	0.972	0.882	26						14 LT
ANKRD12	Chr 18																
9254838	rs199503455	p.Ser524Cys	12	151964	7.90e-5	0.996	0.010	0.864	0.557	0.687	24						9 EU, 2 AA
9255011	rs187421957	p.Arg582Gly	13	151912	8.56e-5	0.962	0.000	0.866	0.727	0.593	24						13 EU
9256635	rs549560546	p.Lys1123Thr	11	152158	7.23e-5	0.994	0.000	0.588	0.742	0.543	26						8 AA, 2 LT, 1 EU
9258816	rs190468609	p.Arg1850His	14	152078	9.21e-5	0.996	0.010	0.466	0.224	0.598	27						5 EU, 5 LT, 3 other, 1 AA
9258843	rs369087314	p.Gln1859Arg	10	152206	6.57e-5	0.969	0.000	0.366	0.224	0.517	26						10 AA
YDH	Chr 2																
31339527	rs142329784	p.Arg1246Cys	66	152202	4.34e-4	0.963	0.000	0.428	0.913	0.312	29						59 EU, 7 AA
31339596	rs116290580	p.Arg1223Cys	15	152202	9.86e-5	0.943	0.000	0.260	0.762	0.388	28						13 AA 2 EU
31339598	rs148235835	p.Thr1222Ile	41	152208	2.69e-4	0.995	0.000	0.470	0.945	0.769	27						34 EU, 6 LT, 1 AA
31339668	rs770434783	p.Ala1199Val	11	152228	7.23e-5	0.929	0.000	0.481	0.941	0.480	26						7 FN, 4 EU
31341378	rs139515054	p.Ile1179Thr	329	152166	2.16e-3	0.976	0.000	0.338	0.844	0.707	28						221 EU, 56 LT, 27AA, 19FN
31348282	rs142402298	p.Thr1045Ala	16	152180	1.05e-4	0.820	0.000	0.399	0.946	0.766	27						16 EU
31349744	rs148921536)	p.Glu971Lys	13	152206	8.54e-5	0.649	0.000	0.167	0.372	0.259	26						11 EU, 1 AA, 1 LT
31350118	rs776794071	p.Arg913Trp	15	152184	9.86e-5	1.000	0.000	0.716	0.979	0.782	26						8 LT, 6 EU, 1 AA
31365991	rs148585342	p.Ala814Val	67	152156	4.40e-4	0.957	0.010	0.295	0.912	0.420	27						47 EU, 16 LT, 3 AA
31366019	rs140007233	p.Arg805Trp	11	152156	7.23e-5	0.998	0.000	0.362	0.942	0.442	27						10 EU, 1 AA
31366070	rs141050887	p.Ile788Phe	122	152064	8.02e-4	0.795	0.000	0.319	0.846	0.341	25						108 EU, 10 AA, 3 LT, 1 SA
31366072	rs149717617	p.Arg787Gln	45	152190	2.96e-4	0.972	0.000	0.209	0.433	0.274	28						25EU, 12LT, 3SA, 2FN, 1AA
31366073	rs148904866	p.Arg787Trp	13	152108	8.55e-5	0.999	0.000	0.380	0.913	0.506	25						5 EA, 4 EU, 4 AA
31366946	rs755854585	p.Cys749Tyr	12	152250	7.88e-5	0.918	0.000	0.259	0.513	0.297	25						6 EU, 6 LT
31368050	rs142848703	p.Ile703Lys	16	152208	1.05e-4	0.935	0.000	0.259	0.695	0.523	27						15 AA, 1 LT
31368056	rs527413763	p.Asp701Val	18	152148	1.18e-4	0.898	0.020	0.328	0.806	0.450	33						17 AA, 1 LT
31372247	rs201668777	p.Arg613Trp	11	152244	7.23e-5	0.803	0.000	0.071	0.873	0.159	23						5 EU, 4 LT, 2 AA
31372358	rs139772558	p.Arg576Trp	234	152204	1.54e-3	0.767	0.000	0.072	0.872	0.277	26						220 AA, 10LT, 1EU 3 other
31375459	rs148603901	p.Arg508Gln	28	152176	1.84e-4	1.000	0.000	0.379	0.928	0.692	26						21 AA, 6 EU, 1 ME
31379899	rs372033714	p.Leu404Met	26	152224	1.71e-4	0.779	0.020	0.158	0.926	0.278	24						24 AA, 2 LT

31383002	rs142388231	p.Ala346Val	40	152142	2.63e-4	0.938	0.000	0.358	0.946	0.620	33	25 EU, 8 AJ, 4 AA, 2 LT
31383080	rs200384255	p.Pro320Arg	19	152198	1.25e-4	0.935	0.000	0.246	0.881	0.361	24	17 EU, 2 AA
31383782	rs138674014	p.Leu287Val	82	152160	5.39e-4	0.754	0.000	0.313	0.922	0.344	23	65 EU, 6 SA, 3 LT, 2 AA
31383785	rs375277410	p.Glu286Gln	29	152196	1.91e-4	0.985	0.010	0.267	0.931	0.421	24	28 AA, 1 LT
31386510	rs149487595	p.Arg233Cys	11	152106	7.23e-5	0.983	0.000	0.205	0.934	0.432	25	8 EU, 3AA
31387845	rs201332711	p.Pro206Leu	28	152150	1.84e-4	1.000	0.000	0.247	0.956	0.351	28	18 EU, 8 AJ, 1 AA, 1 LT
31397681	rs200810102	p.Arg161Gln	13	152158	8.54e-5	0.710	0.010	0.293	0.129	0.431	27	11 LT, 2 EU
31397700	rs145413551	p.Pro155Thr	56	152218	3.68e-4	1.000	0.030	0.309	0.492	0.478	23	49 AA, 5 LT, 2 EU
31398605	rs377748577	p.Pro134Leu	18	152206	1.18e-4	1.000	0.010	0.351	0.709	0.576	25	17 FN, 1 EU
31398642	rs768170843	p.Met122Leu	10	152160	6.57e-5	0.997	0.000	0.303	0.601	0.476	25	9 EU 1 AA
31398678	rs147286954	p.Gly110Ser	15	152160	9.86e-5	0.965	0.000	0.596	0.738	0.503	26	15 LT
31414634	rs773456900	p.Asn11Lys	10	152154	6.57e-5	0.881	0.000	0.372	0.985	0.357	22	8 EU, 1 AA, 1 LT

MTCL1 Chr 18

8705986	rs1000002519	p.Asp109Gly	22	148310	1.48e-4	0.911	0.030	-----	0.461	-----	28	16 EU, 3 AJ, 1 LT
8718626	rs139379863	p.Arg59Gln	24	152198	1.64e-4	0.943	0.000	0.656	0.775	0.455	31	14 EU, 10 LT, 1 AA
8720458	rs150009615	p.Lys107Gln	16	152226	1.05e-4	0.596	0.000	0.585	0.742	0.373	25	14 AJ, 1 EU, 1 other
8783737	rs554525790	p.Leu209Val	15	152140	9.86e-5	0.808	0.000	0.077	0.333	0.231	19	14 AA, 1 LT
8783938	rs145413531	p.Arg276Cys	18	152172	1.18e-4	0.999	1.000	0.158	0.871	0.332	25	15 AA, 2 LT, 1 SA
8784010	rs200271750	p.Arg300Trp	95	152178	6.24e-4	0.978	0.000	0.108	0.717	0.150	28	60 FN, 31 AA, 4 EU
8784055	rs780158820	p.Arg315Trp	14	152166	1.05e-4	0.761	0.000	0.042	0.065	0.112	24	14 AA, 2 EU
8784259	rs367857172	p.Arg383Trp	15	152158	9.86e-5	0.978	0.000	0.182	0.932	0.207	23	10 AA, 3 EU, 1 LT, 1 SA
8784316	rs149027252	p.Arg402Cys	15	152132	9.86e-5	0.961	0.000	0.225	0.797	0.224	23	10 AA, 3 EU, 1 LT, 1 other
8784335	rs372469977	p.Arg408Gln	12	152170	7.89e-5	0.983	0.000	0.207	0.862	0.344	25	10 AJ, 2 AA
8784389	rs140267953	p.Ser426Leu	88	152132	5.78e-4	0.941	0.000	0.229	0.799	0.339	23	59EU, 13LT, 9AA, 4SA, 1EA
8784413	rs201851779	p.Ser434Leu	13	152136	8.54e-5	0.996	0.010	0.239	0.799	0.278	25	7 EU, 3 EA, 2 AA, 1 LT
8784512	rs147236744	p.Thr467Met	43	152164	2.83e-4	0.990	0.010	0.146	0.625	0.111	22	36 AA, 4 EU, 3 LT
8784520	rs201898483	p.Arg470Cys	18	152160	1.18e-4	0.920	0.020	0.268	0.668	0.289	21	11 LT, 7 EU
8784530	rs143105042	p.Thr473Met	61	152162	4.01e-4	0.840	0.030	0.098	0.609	0.038	20	58 LT, 2 LT, 1 other
8784656	rs146651585	p.Ile515Thr	15	152140	9.86e-5	0.647	0.000	0.178	0.609	0.253	25	12 AA, 2LT, 1 other
8784736	rs114113780	p.Pro542Ser	17	152202	1.12e-4	0.708	0.020	0.139	0.668	0.142	23	15 EA, 2 SA
8784793	rs150423289	p.Arg561Trp	35	152214	2.30e-4	0.993	0.000	0.409	0.669	0.409	26	24 EU, 6 SA, 3 LT, 2 AA
8784836	rs375168888	p.Asp575Gly	16	152092	9.20e-5	0.928	0.010	0.373	0.625	0.348	27	12 EU, 1 AA, 1 LT
8786041	rs770066213	p.Gly613Arg	10	151910	6.58e-5	0.760	0.000	0.248	0.654	0.331	23	4 EU, 4 LT, 1 AA, 1 EA
8796356	rs150964075	p.Arg712Gln	35	152142	2.30e-4	0.938	0.000	0.338	0.766	0.307	27	30 EU, 4 AA, 1 other
8807014	rs532812464	p.Ala853Val	12	152184	7.89e-5	0.991	0.000	0.366	0.856	0.187	26	9 EU, 2 AA, 1 SA
8813183	rs139744939	p.Arg937Trp	11	152148	7.23e-5	0.999	0.000	0.428	0.773	0.487	29	9 AA, 1 EU, 1 SA
8824734	rs367681723	p.Arg1075His	10	152132	6.57e-5	0.994	0.000	0.357	0.773	0.292	28	5 EU, 3 AA, 1 LT, 1 other
8824768	rs149983879	p.Lys1086Asn	27	152152	1.77e-4	0.575	0.000	0.106	0.661	0.136	23	24 EU, 3 AA
8824977	rs138372811	p.Tyr1156Cys	12	152180	7.89e-5	0.949	0.020	0.128	0.678	0.231	25	12 AA
8825022	rs149277971	p.Pro1171Leu	14	152234	9.20e-5	0.705	0.000	0.147	0.709	0.352	26	12 EU, 2 AA
8825108	rs781258348	p.Arg1200Cys	14	152188	9.20e-5	0.968	0.030	0.126	0.700	0.314	28	13 AA, 1 EU
8825531	rs144633551	p.Ser1341Gly	49	152182	3.22e-4	0.577	0.000	0.209	0.664	0.265	26	49 AA
8825582	rs116331286	p.Val1358Met	10	152212	6.57e-5	0.869	0.010	0.143	0.496	0.100	24	8 EU, 1 AA, 1 other
8825586	rs116291960	p.Ser1359Leu	75	152198	4.93e-4	0.988	0.000	0.276	0.751	0.385	24	45 EA, 15 AA, 8 LT, 2 SA
8825720	rs371275636	p.Asp1404Asn	11	152156	7.23e-5	0.780	0.000	0.182	0.712	0.249	28	5 AA, 3 LT, 2 EU, 1 other
8825787	rs374048104	p.Arg1426Leu	14	152196	9.20e-5	1.000	0.000	0.481	0.760	0.553	31	13 AJ, 1 EU
8825858	rs114538532	p.Ile1450Val	721	152068	4.74e-3	0.656	0.010	0.066	0.363	0.159	21	423AA,110LT,89SA,60EA,33EU
8825861	rs146614505	p.Asp1451Asn	31	152174	2.04e-4	0.994	0.000	0.404	0.712	0.368	28	29 EU, 1 LT, 1 AA
8825903	rs61753867	p.Arg1465Trp	32	152204	2.10e-4	0.982	0.010	0.189	0.615	0.205	24	23 AJ, 8 EU, 1 AA
8825915	rs372807917	p.Arg1469Trp	21	152238	1.38e-4	0.989	0.000	0.276	0.723	0.281	25	8 EA, 9 AA, 1 EU, 1LT, 1SA
8826092	rs139202553	p.Glu1528Lys	15	152254	9.85e-5	0.999	0.000	0.307	0.828	0.499	29	8 EU, 5 LT, 1 AA, 1 FN
8826105	rs574852095	p.Arg1532Gln	17	152224	1.12e-4	0.999	0.000	0.349	0.828	0.500	31	5 SA, 5 EU, 4 EA, 2AA, 1LT
8831796	rs201909742	p.Arg963Ter	10	152152	6.57e-5	Stop gained	1998/2011					8 AA, 2 EU

TSPYL2 Chr X

53082628	rs782451065	p.Gln44Glu	23	111425	2.06e-4	0.596	0.010	0.094	0.731	0.091	22	20 EU, 2 FN, 1 AA
53085058	rs781934817	p.Phe368Ile	12	112446	1.07e-4	0.994	0.000	0.436	0.934	0.565	26	12 EU

Many in-frame deletions of unknown effect

FOXR2 Chr X

55624507	rs374320995	p.Arg266Cys	14	112660	1.24e-4	0.097	0.020	0.727	0.773	0.375	10	10 EU, 1 AA, 1 LT, 1 EA
55624623	rs745397944	p.Leu304Phe	10	112848	8.86e-5	0.582	0.000	0.680	0.261	0.237	18	5 SA, 5 EA

-
1. Lucitti JL, Sealock R, Buckley BK, et al. Variants of Rab GTPase-effector binding protein-2 cause variation in the collateral circulation and severity of stroke. *Stroke* 2016; 47: 3022-3031.
 2. Clayton JA, Chalothorn D, Faber JE. Vascular endothelial growth factor-A specifies formation of native collaterals and regulates collateral growth in ischemia. *Circ Res* 2008; 103: 1027-1036.
 3. Lucitti JL, Mackey J, Morrison J, et al. Formation of the collateral circulation is regulated by vascular endothelial growth factor-A and A Disintegrin and Metalloprotease Family Members 10 and 17. *Circ Res* 2012; 111: 1539-1550.
 4. Cristofaro B, Shi Y, Faria M, et al. Dll4-Notch signaling determines the formation of native arterial collateral networks and arterial function in mouse ischemia models. *Development* 2013; 140: 1720-1729.
 5. Okyere B, Giridhar K, Hazy A, et al. Endothelial-specific EphA4 negatively regulates native pial collateral formation and re-perfusion following hindlimb ischemia. *PLoS One* 2016; 11: e0159930.
 6. Chalothorn D, Zhang H, Smith JE, et al. Chloride intracellular channel-4 is a determinant of native collateral formation in skeletal muscle and brain. *Circ Res* 2009; 105: 89-98.
 7. Lucitti JL, Tarte NJ, Faber JE. Chloride intracellular channel-4 is required for maturation of the cerebral collateral circulation. *Am J Physiol Heart Circ Physiol* 2015; 309: H1141-H1150.
 8. Fang JS, Angelov SN, Simon AM, et al. Cx37 deletion enhances vascular growth and facilitates ischemic limb recovery. *Am J Physiol Heart Circ Physiol* 2011; 301: H1872-H1881.

Bioinformatic analysis of prioritized candidate genes' functions, expression in vascular tissues/cells, and evidence suggesting potential involvement in the collateralogenesis pathway.

The following websites (underlined) and references therein were examined for the genes in Table 1 to query their functions, mutants, expression by vascular cells/tissues, etc, ascertained in mouse (M) and human (H). We relied in particular on information provided in the sections within the sites given in brackets: Ensemble-UniProtKB: Function/Induction, Subcellular location, Expression (in vascular tissues, endothelial and smooth muscle cells) [Bgee, Genevisible (GV)], Protein-protein interactions [STRING], Genetic variation; MGI (M): Mutations, Alleles, Phenotypes; Alliance-Gene page (M): Description, Phenotypes, Disease associations, Alleles and variants, Models (KO, Tg, etc); HGCN-Genecards (H): Summaries/descriptions, Function [GWAS Catalog, Phenotypes, Animal models], Variants, Disorders, Localization, Expression in vascular tissues and cells [GTEX, HPA], Pathways; NCBI Gene (M/H); Medline/Pubmed (M/H).

Canq5:

Sox13, SRY-Box Transcription Factor 13, a SOX family whose members regulate embryonic development and cell fate, is involved in T-cell development and brown adipocyte differentiation, and inhibits Wnt signaling. It has recently been linked to angiogenesis in gliomas and promotes angiogenesis on forced expression in glioma endothelial cells.¹ Expression in mouse is very high in embryonic arteries² and embryonic lung endothelial cells and intermediate in arteries and kidney vasculature of adults, compared to other tissue/cell types, while in adult human it is very high in arteries, endothelial and smooth muscle cells (Bgee, GV, GTEX, HPA). The above findings support a potential role for Sox13 in collateralogenesis.

Cyb5r1, cytochrome b5 reductase 1, is an NADH-cytochrome b5 reductase that is localized to the plasmalemma, mitochondria and endoplasmic reticulum. Cyb5r family members are involved in desaturation and elongation of fatty acids, cholesterol biosynthesis, drug metabolism, and EMT and the infiltrative tumor cell phenotype in colon cancer.³ Expression in mouse and human is intermediate in brain vessels, aorta, arteries, veins, endothelial and smooth muscle cells (Bgee, GV, GTEX, HPA), compared to other tissue/cell types. Cyb5r1 is also responsible for reduction of methemoglobin, which in its oxidized form is defective in binding oxygen. Loss of function variants of Cyb5r1 cause familial methemoglobinemia and susceptibility to functional anemia and tissue hypoxia. Cyb5r1 is upregulated in diabetic retinopathy which is accompanied by hypoxia-induced pathological angiogenesis.⁴ These findings suggest Cyb5r1 may play a role in the hypoxia→VEGFA→Flk1→Rabep2 component of the collateralogenesis signaling pathway. However, Cyb5r2 was also shown to be upregulated in diabetic retinopathy, but unlike above,⁴ inhibited angiogenesis in vitro,⁵ and to act as a tumor suppressor in nasopharyngeal carcinoma by attenuating angiogenesis.⁶

Rgs1, regulator of G-protein signaling-1, is a GTPase-activating protein that limits G_{α} and $G_{\beta\gamma}$ signaling from certain G protein-coupled receptors (GPCRs).⁷ Deficiency in *Rgs1* has been linked to abnormal trafficking of immunoglobulin-secreting cells and autoimmune-like disease. However little information exists regarding its role in vascular development. Expression is intermediate in arteries, ECs, and smooth muscle cells of mouse and human.⁸ (see also Bgee, Genevisible) Knockout/down of *Rgs1* suppressed angiogenesis in a rat model of arthritis⁹ and reduced expression of VEGF, proliferation of ECs, and neovascularization in the ischemic mouse choroid.¹⁰ These reports are consistent with our finding that wildtype (B6 allele) AAV9-*Rgs1* induced collateral formation in CC016 mice and conclusion that deficient Rgs1 activity

contributes to reduced collateralogenesis and the sparse collaterals evident in CC016 mice. However, findings from other studies could suggest that increased signaling by GPCRs that contribute to collateralogenesis, resulting from interacting with a deficient Rgs1, would be expected to lead to *more* abundant collaterals in CC016, and therefore that wildtype AAV9-*Rgs1* should have had no effect (or decreased collateral number if the latter exhibits competitive binding): SDF1→CXCR4 signaling, which is limited by Rgs1,⁷ promotes formation of a collateral pathway after arterial occlusion of the dorsal aorta in zebrafish¹¹ and additional collaterals in the newborn heart¹² and adult brain¹³ of mice exposed to prolonged hypoxemia. Also, hypoxia reportedly increased RGS1 expression through a HIF-dependent mechanism, resulting in dampening of SDF1-induced migration of human mesenchymal stem cells¹⁴—cells which have been shown to be involved in collateral formation in adult heart.¹⁵ In addition, sphingosine-1-phosphate (S1P) which interacts with Rgs1⁹ has been implicated in formation of arteriole anastomoses induced by an S1P receptor agonist in the mouse dorsal skin fold chamber¹⁶ and formation of additional collaterals following MCA occlusion.¹⁷⁻¹⁹ Of note, pharmacological inhibition of angiotensin converting enzyme induced the formation of arterial anastomoses in chick embryo, leading to the possibility that on or both of the GPCR activating ligands, angiotensin and kallikrein, is involved in collateralogenesis;²⁰ however AT1 receptor signaling is strongly restrained by Rgs8 rather than by Rgs1.²¹ Resolution of the above disparate findings vis-à-vis collateralogenesis awaits additional investigation.

Aspm, abnormal spindle microtubule assembly, which is located in the cytoplasm and nucleus, is involved in mitotic spindle regulation with a preferential role in neurogenesis. Expression of *Aspm* in mouse and human is low in blood vessels (Bgee, GTEEx, HPA) with the exception of being very high in choroid and iris microvessel endothelial cells (GV-H). KO mice evidence severe microcephaly.

Cfhr1 and Cfhr4, complement factor H-related 1 and 4, respectively, are secreted plasma proteins synthesized primarily by hepatocytes. They are involved in complement regulation, and can associate with lipoproteins and may participate in lipid metabolism. Mutations, primarily linked to age-related macular degeneration, have not been associated with any vascular phenotype; KO models has not been reported. *Cfhr1* is expressed at high levels in coronary artery, aorta, aorta and smooth muscle and endothelial cells (Bgee-H, GV-H, HPA), compared to other tissues/cell types. *Cfhr4* is expressed at intermediate levels in aorta, coronary and tibial arteries, endothelial cells and human blood outgrowth endothelial cells (Bgee-H, GV-H, HPA). No publications for either protein have reported involvement in vessel formation or function.

Canq6:

Jak3, Janus kinase 3, is a non-receptor tyrosine kinase involved in cell growth, development, differentiation, T- and B-cell development, and signaling in innate and adaptive immunity--in particular by type I interleukin receptors and other cell surface receptors to downstream effectors including STAT proteins which activate gene expression. Mutations in humans are associated with severe combined immunodeficiency disease, and point mutations in mice develop autoimmune inflammatory bowel disease and altered susceptibility to malaria and bacterial infection. *Jak3* is expressed predominantly in immune cells. Expression is low in mouse vessels (Bgee, GV) and in human is intermediate in aorta and high in temporal and coronary arteries and endothelial and smooth muscle cells (Bgee, GTEEx, HPA). *Jak3* negatively regulated re-endothelialization, endothelial proliferation, and proliferation and alpha-actin expression in intimal cells after wire injury of the carotid artery.²² Consistent with Jak-STAT signaling in hypoxic

Hif1 α -mediated induction of several angiogenic genes, Jak3 is required for VEGFA-mediated proliferation, migration and angiogenesis in human microvascular endothelial cells.²³ It also regulates adherens junctions and epithelial mesenchymal transition through β -catenin.²⁴ The above findings support a potential role for Jak3 in collaterogenesis.

Yjefn3, Yjef N-terminal domain containing 3 (ApoA-I binding protein 2), binds ApoA-I on HDL and accelerates cholesterol efflux from endothelial cells to high-density lipoprotein (HDL). It also activates endothelial SREBF2, the master transcription factor for cholesterol biosynthesis, which in turn transactivates Notch and promotes hematopoietic stem and progenitor cell emergence from the hemogenic endothelium.²⁵ Increased Yjefn3 was shown to interfere with VEGF-R2 dimerization and VEGFA induced angiogenesis in mouse endothelial cells and to inhibit angiogenesis in zebrafish, whereas knockdown of Yjefn3 in the latter resulted in dysregulated sprouting/branching angiogenesis. These results indicate biphasic effects on embryonic angiogenesis depending on Yjefn3 level.^{25,26} Expression in adult mice and humans is low in arteries, veins, endothelial and smooth muscle cells (Bgee, GV, GTEx, HPA). The above data suggest that Yjefn3 may play a role in collaterogenesis.

Not entries are given herein for the last 6 genes in Table 1 for *Canq6* because each was deemed very unlikely to be involved in collaterogenesis based on the following: highly restricted expression and function in cell types unlikely to be involved in collaterogenesis (Bgee, Genevisible (GV); the Pubmed search terms angiogenesis, vascular development, endothelial cell function, and endocytic vesicle trafficking did not return references.

Canq7:

Cav2, caveolin-2, forms a stable complex with caveolin-1 to target lipid rafts and caveolae formation which regulate endocytic vesicle trafficking. It is involved in essential cellular functions, including signal transduction, lipid metabolism, cellular growth control and apoptosis. Caveolin-2 (and caveolin-1) also binds G-protein alpha subunits and can regulate their activity, promotes Src-mediated phosphorylation and binding of Ras1, Src and Nck1, colocalizes with focal adhesions where it links integrin subunits (including β 3 on endothelial cells) to the tyrosine kinase FYN, is an initiating step in coupling integrins to the Ras-ERK pathway, and binds to endothelial cell NOS3 (eNOS) and promotes NO production. Caveolin-2 also induces nuclear translocation of Stat3,²⁷ and modulates endothelial cell proliferation: KO mice exhibit increased proliferation of endothelial cells in lung in association with loss of an inhibitory effect of caveolin-2 on TGF- β --Smad2/3 signaling (through internalization of TGFBR1 from membrane rafts and subsequent degradation).^{28,29} On the other hand, reduced angiogenesis and growth of subcutaneously implanted tumors was observed in KO mice³⁰—responses also seen in caveolin-1 KO mice.³¹ Although not significant, infarct volume after permanent MCA occlusion was 30% lower in *Cav2* KO than wildtype mice, whereas it was significantly increased by 88% in *Cav1* KOs (n=10-16 per group).³² Interestingly, a SNP in the 3'UTR of *CAV2*, rs4727833, has been linked to cardioembolic stroke (P-value 2×10^{-7} , OR 1.09, CI 1.06-1.13, MAF 0.45);³³ This SNP is in linkage disequilibrium (r^2 0.96, MAF 0.45) with an intergenic SNP for *CAV2* that has been linked in three other GWAS studies to atrial fibrillation (P-value 7×10^{-13}), heart rate response to exercise (P-value 2×10^{-9}) and heart rate response to recovery post exercise (P-value 7×10^{-10}) (GWAS Catalog); these SNPs have eQTLs for increased expression of *CAV2* by tibial artery (2.7×10^{-10} and 1.2×10^{-9} , respectively, both with normalized effect size 0.23) (GTEx); Differences in coronary collateral status, which evidence suggests may cause differences in tissue oxygen delivery during increases in oxygen demand,³⁴ could contribute to these traits. Expression of

Cav2 is very high in mouse brain microvessels and aorta (Bgee, GV) and in human arteries, veins, endothelial and smooth muscle cells (Bgee, CV, HPA). The above findings support a potential role for caveolin-2 in collaterogenesis.

Iqub, IQ motif and ubiquitin domain containing, is found in the cytoplasm and nucleoplasm, especially in sperm cells. Two publications have investigated the function of Iqub: One tested siRNA against expression of putative cilia genes in cell lines with findings suggesting it may play a role in primary cilium assembly or maintenance and in hedgehog signaling.³⁵ A second study found that Iqub was upregulated in breast cancer and promoted proliferation and migration of a breast cancer cell line via activating Akt/GSK3 β /Wnt/ β -catenin signaling.³⁶ In mouse and human, expression is high in sperm, ciliated respiratory and endometrial cells, very low in other tissues including brain vessels and aorta, and not detected in endothelial and smooth muscle cells (Bgee, GTE_x, HPA).

Canq8:

Pld1, phospholipase D1, which is selective for phosphatidylcholine, is stimulated by PIP₂ and PIP₃, and to a lesser degree by RhoA, Rac1 and CDC42. Pld1 is localized to the plasma membrane, endosomes, golgi, endoplasmic reticulum, and perinuclear area, and is an important element in numerous cellular pathways including receptor signal transduction, vesicle trafficking at the plasma and nuclear membranes, and regulation of mitosis. Endothelial cells deficient in Pld1 show reduced PI3K-Akt and MEK-ERK signaling in response to FLK1/VEGFR2 activation, reduced integrin-dependent adhesion, migration, and proliferation, and reduced angiogenesis in vitro, in tumor xenographs, hypoxic retina, and in zebrafish during development.³⁷⁻³⁹ Expression in mouse is intermediate in carotid and brain vessels (Bgee) and in human is intermediate in aorta, carotid and tibial arteries, endothelial and smooth muscle cells, low in saphenous vein (Bgee, HPA) and is very high in blood outgrowth endothelial cells (GV). The above findings suggest that Pld1 may play a role in collaterogenesis.

Fat4, FAT atypical cadherin 4, which localizes to the plasma membrane and primary cilia, is involved in cell junctions and adhesion, planar cell polarity, receptor and YAP1-hippo signaling, neuroprogenitor and mesenchymal cell proliferation, and development including that of the lymphatic vasculature through a lymphatic endothelial cell autonomous manner.⁴⁰ KO mice show neonatal lethality with reduced body size and altered morphology in several non-vascular tissue types. Recent evidence suggests a role for Fat4 in pericyte differentiation and proliferation.⁴¹ Expression in mouse is very high in carotid, aorta and brain vessels (Bgee) and in human is very high in aorta, popliteal, tibial and coronary arteries, endothelial and blood outgrowth endothelial cells and vascular smooth muscle cells (Bgee, GV, GTE_x, HPA). The above findings suggest Fat4 may be involved in collaterogenesis.

Usp13, ubiquitin specific peptidase 13 (isopeptidase T-3), is located in the cytosol and nucleus. Usp13 deubiquitinates BECN1, MITF, SKP2, USP10 and other proteins and is involved in autophagy and endoplasmic reticulum-associated degradation. Among its binding partners is the dual specificity phosphatase PTEN. In mouse lung fibroblasts, USP13 appears to regulate stability of Smad 4 leading to ECM expression and cell differentiation, and both translocate to the cytoplasm in response to TGF- β 1.⁴² Expression in mouse is intermediate in aorta and carotid artery (Bgee), while in human it is high in vena cava, saphenous vein, smooth muscle and endothelial cells, intermediate in temporal and popliteal arteries, and low in coronary artery and aorta (Bgee, HPA, GTE_x).

GM1527, predicted gene 1527, is predicted to activate small GTPases. Expression in mouse is restricted to morula blastoderm and sperm cells (Bgee). No information exists for this gene in human, and Pubmed lists no functional information.

Canq9:

Arhgap28, Rho GTPase activating protein 28, which resides primarily in the cytoplasm, negatively regulates RhoA signaling which has a number of downstream effectors including stress fiber assembly. There are no reports examining Arhgap28 in vascular wall cells. In one KO mouse model, blood vessel development was impaired and early postnatal lethality occurred. In another, KOs were viable and appeared normal, however an increase in the closely related Arhgap6 led the authors to suggest that it may have compensated for loss of Arhgap28.⁴³ Arhgap28 interacts in protein binding assays with Arhgap29 (STRING). Expression of the latter was recently found to be induced during lumenization of endothelial cell cords early in vascular development, and through its inhibition of RhoA, to interfere with non-muscle myosin II mediated generation of endothelial cell tension, resulting in maintenance of lumen formation (Ondine Cleaver, pers comm). It is possible that Arhgap28 may assist Arhgap29 in the above and contribute to collaterogenesis. Consistent with the above findings, *Arhgap28* is expressed at high levels in mouse carotid artery, brain vessels, endothelial cells and smooth muscle cells, compared to other tissues (Bgee). In human, it is expressed at high levels in endothelial and smooth muscle cells, and at intermediate levels in tibial, coronary and hepatic arteries and saphenous vein, compared to low levels in other tissues (excepting sperm, lungs and kidney glomerulus where expression is high) (Bgee, GV, HPA).

Rmdn2, regulator of microtubule dynamics 2, binds with microtubules and presumably influences their functions, including chromosomal segregation in *C elegans*.⁴⁴ However, little is known about Rmdn2 function aside of its association with amyotrophic lateral sclerosis and congenital glaucoma. Located in the cytoplasm, its expression in mice is low in aorta, carotid artery and brain vessels (Bgee), while in human levels are moderate in aorta, coronary artery, endothelial and smooth muscle cells (Bgee, GTEEx, HPA), compared to other tissues and cell types.

Myom1, myomesin (skelemin), binds myosin, meromyosin, and titin in striated muscle where it is thought to link intermediate filaments to the M-disk. It also binds probable hydrolase PNKD which can activate the NF-kappa-B signaling pathway, binds $\beta 1/\beta 3$ integrins which are important in angiogenesis during development, and is present in endothelial cells.^{45,46} Myomesin is also found in the nucleus where it affects gene expression.⁴⁵ In mouse, *myomesin* is expressed at intermediate levels in aorta, carotid artery, and brain blood vessels (Bgee) and in human at high levels in coronary and tibial arteries, intermediate levels in aorta and vena cava, and at very high levels in striated muscle, smooth muscle, and endothelial cells (GTEEx, Bgee, HPA) compared to other cell types. The above findings support a possible role for myomesin in collaterogenesis.

No entries are given herein for Ankrd12, Xdh and Mtcl1 for *Canq9* because each was deemed very unlikely to be involved in collaterogenesis based on the following: highly restricted expression and function in cell types unlikely to be involved in collaterogenesis (Bgee, Genevisible (GV); the Pubmed search terms angiogenesis, vascular development, endothelial cell function, and endocytic vesicle trafficking did not return references.

Canq10:

Tspyl2, Testis-specific Y-encoded-like protein 2, is subject to x-inactivation, resides in the nucleolus and at lower levels in the cytoplasm, participates in nucleosome assembly, modulates transcription including glutamate receptor expression in embryonic brain, inhibits cell-cycle progression and is involved in embryonic stem cell differentiation. It is ligated by TGF β 1, and is involved in both the canonical (Smad-based) and noncanonical TGF β signaling pathways,⁴⁷ the latter activating MAPKs including ERK, p38, and JNK, and that it signals to PI3K-AKT and Rho-like GTPases.⁴⁸ *Tspyl2* is induced in a hypoxia-inducible factor-1 α (Hif1 α)-dependent manner⁴⁹ and augments TGF β signaling in vascular wall cells.⁵⁰ The above pathways are important in vasculogenesis and angiogenesis during development. Experimentally induced diabetes upregulated vascular *Tspyl2*, it is upregulated in human diabetic aorta, and deletion in diabetic mice promotes aorta aneurysm formation and reduced diabetes-induced accumulation of kidney collagen III and IV and tubular injury. Its pro-fibrotic activity is mediated through cross-talk with TGF β and negatively regulates NF- κ B signaling.^{48,50-53} The above support a possible role for *Tspyl2* in collaterogenesis. Reinforcing this, mouse *Tspyl2* is widely expressed among tissues from embryonic day E10.5 to P7, including in brain, and at intermediate levels in arteries and brain blood vessels in adult (Bgee, GV). Human *TSPYL2* expression is moderately high in arteries, smooth muscle, and endothelial cells (GTEx, Bgee, HPA). One KO mouse model was embryonic lethal, while another resulted in behavioral and brain morphological alterations that mirror a number of neurodevelopmental psychiatric traits.

Foxr2, forkhead box R2, a member of the Fox family of transcription factors, resides at low levels in the nucleoplasm, is expressed at low levels in all tissues and cells (Bgee, GV, GTEx, HPA), and is involved in embryogenesis, differentiation, epithelial-mesenchymal transformation and metabolism. Foxr2 induces expression of sonic hedgehog which is important in early vascular development, stimulates angiogenesis in association with increased VEGF-A expression, promotes tumor progression, and is aberrantly expressed in a variety of cancers at levels that correlate with cancer progression⁵⁴⁻⁵⁶. Downregulation of Foxr2 strongly reduced Shh, Gli1, and Ptch1 protein in a tumor cell line.⁵⁴ In glioma endothelial cells, Foxr2 ligated the promoters and increased expression of ZO-1 and claudin-5.⁵⁷ Foxr2 was also shown to activate FAK/SRC signaling in brain tumor cells.⁵⁸ All of the above signals are involved in vasculogenesis and angiogenesis during development, consistent with a potential contribution of Foxr2 to collaterogenesis.

Genes in Supplemental table III that were subjected to in vivo AAV9 assay:

Cxcr4, chemokine (C-X-C motif) receptor 4. See Rgs1, above, for rationale for this gene's rank and selection for testing.

C1galt1, core 1 synthase, glycoprotein-N-acetylgalactosamine 3-beta-galactosyltransferase 1, is plasma lemma protein that is a precursor for many extended O-glycans in glycoproteins, and has a central role in many processes, including angiogenesis and thrombopoiesis. Xia et al⁵⁵ found that expression in mice is primarily in endothelial, hematopoietic, and epithelial cells during development. They also reported that KO mice develop brain hemorrhage that was uniformly fatal by embryonic day 14, with chaotic microvascular networks in brain, distorted capillary lumens and defective association of endothelial cells with pericytes and extracellular matrix. The above findings support a possible role for C1galt1 in collaterogenesis.

References

1. O'Brien JB, Wilkinson JC, Roman DL. Regulator of G-protein signaling (RGS) proteins as drug targets: Progress and future potentials. *J Biol Chem* 2019; 294: 18571-18585.
2. Cho H, Harrison K, Schwartz O, et al. The aorta and heart differentially express RGS (regulators of G-protein signaling) proteins that selectively regulate sphingosine 1-phosphate, angiotensin II and endothelin-1 signaling. *Biochem J* 2003; 371: 973-980.
3. Hu X, Tang J, Zeng G, et al. RGS1 silencing inhibits the inflammatory response and angiogenesis in rheumatoid arthritis rats through the inactivation of Toll-like receptor signaling pathway. *J Cell Physiol* 2019; 234: 20432-20442.
4. Zhang Q, Zhang F, Guo Y, et al. Regulator of G-protein signaling 1 promotes choroidal neovascularization in age-related macular degeneration. *Ann Transl Med* 2022; 10: 982.
5. Packham IM, Gray C, Heath PR, et al. Microarray profiling reveals CXCR4a is downregulated by blood flow in vivo and mediates collateral formation in zebrafish embryos. *Physiol Genomics* 2009; 38: 319-327.
6. Das S, Goldstone AB, Wang H, et al. A unique collateral artery development program promotes neonatal heart regeneration. *Cell* 2019; 176: 1128-1142.
7. Zhang H, Rzechorzek W, Aghajanian A, et al. Hypoxemia induces de novo formation of cerebral collaterals and lessens the severity of ischemic stroke. *J Cere Blood Flow Metab* 2020; 40: 1806–1822.
8. Wierenga AT, Vellenga E, Schuringa JJ. Convergence of hypoxia and TGF β pathways on cell cycle regulation in human hematopoietic stem/progenitor cells. *PLoS One* 2014; 9: e93494.
9. Zhang H, Faber JE. De-novo collateral formation following acute myocardial infarction: Dependence on CCR2+ bone marrow cells. *J Molec Cell Cardiol* 2015; 87: 4-16.
10. Sefcik LS, Aronin CE, Awojoodu AO, et al. Selective activation of sphingosine 1-phosphate receptors 1 and 3 promotes local microvascular network growth. *Tissue Eng Part A* 2011; 17: 617-629.
11. Iwasawa E, Ishibashi S, Suzuki M, et al. Sphingosine-1-phosphate receptor 1 activation enhances leptomeningeal collateral development and improves outcome after stroke in mice. *J Stroke Cerebrovasc Dis* 2018; 27: 1237-1251.
12. Nitzsche A, Poittevin M, Benarab A, et al. Endothelial S1P₁ signaling counteracts infarct expansion in ischemic stroke. *Circ Res* 2021; 128: 363-382.
13. Yu F, Feng X, Li X, et al. Association of plasma metabolic biomarker sphingosine-1-phosphate with cerebral collateral circulation in acute ischemic stroke. *Front Physiol* 2021; 12: 720672.
14. le Noble FA, Kessels-van Wylick LC, Hacking WJ, et al. The role of angiotensin II and prostaglandins in arcade formation in a developing microvascular network. *J Vasc Res* 1996; 33: 480-488.
15. Song D, Nishiyama M, Kimura S. Potent inhibition of angiotensin AT1 receptor signaling by RGS8: importance of the C-terminal third exon part of its RGS domain. *J Recept Signal Transduct Res* 2016; 36: 478-487.

16. He Z, Ruan X, Liu X, et al. FUS/circ_002136/miR-138-5p/SOX13 feedback loop regulates angiogenesis in Glioma. *J Exp Clin Cancer Res* 2019 8; 38: 65.
17. Roose J, Korver W, Oving E, et al. High expression of the HMG box factor sox-13 in arterial walls during embryonic development. *Nucleic Acids Res* 1998; 26: 469-476.
18. Woischke C, Blaj C, Schmidt EM, et al. CYB5R1 links epithelial-mesenchymal transition and poor prognosis in colorectal cancer. *Oncotarget* 2016; 7: 31350-31360.
19. Peng L, Ma W, Xie Q, et al. Identification and validation of hub genes for diabetic retinopathy. *PeerJ* 2021; 9: e12126.
20. Chen J, Liao L, Xu H, et al. Long non-coding RNA MEG3 inhibits neovascularization in diabetic retinopathy by regulating microRNA miR-6720-5p and cytochrome B5 reductase 2. *Bioengineered* 2021; 12: 11872-11884.
21. Ming H, Lan Y, He F, et al. Cytochrome b5 reductase 2 suppresses tumor formation in nasopharyngeal carcinoma by attenuating angiogenesis. *Chin J Cancer* 2015; 34: 459-467.
22. Wang YC, Cai D, Cui XB, et al. Janus Kinase 3 Deficiency Promotes Vascular Reendothelialization-Brief Report. *Arterioscler Thromb Vasc Biol* 2021; 41: 2019-2026.
23. Di Benedetto P, Ruscitti P, Berardicurti O, et al. Blocking Jak/STAT signaling using tofacitinib inhibits angiogenesis in experimental arthritis. *Arthritis Res Ther* 2021; 23: 213.
24. Mishra J, Das JK, Kumar N. Janus kinase 3 regulates adherens junctions and epithelial mesenchymal transition through β -catenin. *J Biol Chem* 2017; 292: 16406-16419.
25. Gu Q, Yang X, Lv J, et al. AIBP-mediated cholesterol efflux instructs hematopoietic stem and progenitor cell fate. *Science* 2019; 363: 1085-1088.
26. Fang L, Choi SH, Baek JS, et al. Control of angiogenesis by AIBP-mediated cholesterol efflux. *Nature* 2013; 498: 118-122.
27. Kwon H, Jeong K, Hwang EM, et al. Caveolin-2 regulation of STAT3 transcriptional activation in response to insulin. *Biochim Biophys Acta* 2009; 1793: 1325-1333.
28. Razani B, Wang XB, Engelman JA, et al. Caveolin-2-deficient mice show evidence of severe pulmonary dysfunction without disruption of caveolae. *Mol Cell Biol* 2002; 22: 2329-2334.
29. Xie L, Vo-Ransdell C, Abel B, et al. Caveolin-2 is a negative regulator of anti-proliferative function and signaling of transforming growth factor- β in endothelial cells. *Am J Physiol Cell Physiol* 2011; 301: C1161-1174.
30. Liu Y, Jang S, Xie L, Sowa G. Host deficiency in caveolin-2 inhibits lung carcinoma tumor growth by impairing tumor angiogenesis. *Cancer Res* 2014; 74: 6452-6462.
31. Woodman SE, Ashton AW, Schubert W, et al. Caveolin-1 knockout mice show an impaired angiogenic response to exogenous stimuli. *Am J Pathol* 2003; 162: 2059-2068.
32. Jasmin JF, Malhotra S, Singh Dhallu M, et al. Caveolin-1 deficiency increases cerebral ischemic injury. *Circ Res* 2007; 100: 721-729.
33. Malik R, Chauhan G, Traylor M, et al. Multiancestry genome-wide association study of 520,000 subjects identifies 32 loci associated with stroke and stroke subtypes. *Nat Genet* 2018; 50: 524-537.

34. Faber JE, Storz JF, Chevron ZA, et al. High-altitude rodents have abundant collaterals that protect against tissue injury after cerebral, coronary and peripheral artery occlusion. *J Cere Blood Flow Metab* 2020; 41: 731–744.
35. Lai CK, Gupta N, Wen X, et al. Functional characterization of putative cilia genes by high-content analysis. *Mol Biol Cell* 2011; 22: 1104-1119.
36. Li K, Ma YB, Zhang Z, et al. Upregulated IQUB promotes cell proliferation and migration via activating Akt/GSK3 β / β -catenin signaling pathway in breast cancer. *Cancer Med* 2018; 7: 3875-3888.
37. Chen Q, Hongu T, Sato T, et al. Key roles for the lipid signaling enzyme phospholipase d1 in the tumor microenvironment during tumor angiogenesis and metastasis. *Sci Signal* 2012; 5: ra79.
38. Zhang Q, Wang D, Singh NK, et al. Activation of cytosolic phospholipase A2 downstream of the Src-phospholipase D1 (PLD1)-protein kinase C γ (PKC γ) signaling axis is required for hypoxia-induced pathological retinal angiogenesis. *J Biol Chem* 2011; 286: 22489-22498.
39. Zeng XX, Zheng X, Xiang Y, et al. Phospholipase D1 is required for angiogenesis of intersegmental blood vessels in zebrafish. *Dev Biol* 2009; 328: 363-376.
40. Betterman KL, Sutton DL, Secker GA, et al. Atypical cadherin FAT4 orchestrates lymphatic endothelial cell polarity in response to flow. *J Clin Invest* 2020; 130: 3315-3328.
41. Suo L, Liu C, Zhang QY, et al. METTL3-mediated N⁶-methyladenosine modification governs pericyte dysfunction during diabetes-induced retinal vascular complication. *Theranostics* 2022; 12: 277-289.
42. Liao X, Li Y, Liu J, et al. Deubiquitinase USP13 promotes extracellular matrix expression by stabilizing Smad4 in lung fibroblast cells. *Transl Res* 2020; 223: 15-24.
43. Yeung CY, Taylor SH, Garva R, et al. Arhgap28 is a RhoGAP that inactivates RhoA and downregulates stress fibers. *PLoS One* 2014; 9: e107036.
44. Oishi K, Okano H, Sawa H. RMD-1, a novel microtubule-associated protein, functions in chromosome segregation in *Caenorhabditis elegans*. *J Cell Biol* 2007; 179: 1149-1162.
45. Reddy KB, Gascard P, Price MG, et al. Identification of an interaction between the m-band protein skelemin and beta-integrin subunits. Colocalization of a skelemin-like protein with beta1- and beta3-integrins in non-muscle cells. *J Biol Chem* 1998; 273: 35039-35047.
46. Gorbatyuk V, Nguyen K, Podolnikova NP, et al. Skelemin association with α IIb β 3 integrin: a structural model. *Biochemistry* 2014; 53: 6766-6775.
47. Li J, Huynh P, Dai A, et al. Diabetes reduces severity of aortic aneurysms depending on the presence of cell division autoantigen 1 (CDA1). *Diabetes* 2018; 67: 755-768.
48. Chen L, Wu J, Hu B, et al. The role of cell division autoantigen 1 (CDA1) in renal fibrosis of diabetic nephropathy. *Biomed Res Int* 2021; 2021: 6651075.
49. Xie H, Xu G, Gao Y, et al. hCINAP serves a critical role in hypoxia-induced cardiomyocyte apoptosis via modulating lactate production and mitochondrial-mediated apoptosis signaling. *Mol Med Rep* 2021; 23: 109.
49. Xie H, Xu G, Gao Y, et al. hCINAP serves a critical role in hypoxia-induced cardiomyocyte apoptosis via modulating lactate production and mitochondrial-mediated apoptosis signaling. *Mol Med Rep* 2021; 23: 109.

50. Chai Z, Dai A, Tu Y, et al. Genetic deletion of cell division autoantigen 1 retards diabetes-associated renal injury. *J Am Soc Nephrol* 2013; 24: 1782-1792.
51. Qu L, Ji Y, Zhu X, Zheng X. hCINAP negatively regulates NF- κ B signaling by recruiting the phosphatase PP1 to deactivate IKK complex. *J Mol Cell Biol* 2015; 7: 529-542.
52. Oh BH, Tu Y, Cao Z, et al. Role of cell division autoantigen 1 (CDA1) in cell proliferation and fibrosis. *Genes (Basel)* 2010; 1: 335-348.
53. Epping MT, Lunardi A, Nachmani D, et al. TSPYL2 is an essential component of the REST/NRSF transcriptional complex for TGF β signaling activation. *Cell Death Differ* 2015; 22: 1353-1362.
54. Lu SQ, Qiu Y, Dai WJ, et al. FOXR2 promotes the proliferation, invasion, and epithelial-mesenchymal transition in human colorectal cancer cells. *Oncol Res* 2017; 25: 681-689.
55. Li B, Huang W, Cao N, et al. Forkhead-box R2 promotes metastasis and growth by stimulating angiogenesis and activating hedgehog signaling pathway in ovarian cancer. *J Cell Biochem* 2018; 119: 7780-7789.
56. Liao CW, Zheng C, Wang L. Down-regulation of FOXR2 inhibits hypoxia-driven ROS-induced migration and invasion of thyroid cancer cells via regulation of the hedgehog pathway. *Clin Exp Pharmacol Physiol* 2020; 47: 1076-1082.
57. Leng X, Ma J, Liu Y, et al. Mechanism of piR-DQ590027/MIR17HG regulating the permeability of glioma conditioned normal BBB. *J Exp Clin Cancer Res* 2018; 37: 246.
58. Beckmann PJ, Larson JD, Larsson AT, et al. *Sleeping Beauty* insertional mutagenesis reveals important genetic drivers of central nervous system embryonal tumors. *Cancer Res* 2019; 79: 905-917.
59. Xia L, Ju T, Westmuckett A, et al. Defective angiogenesis and fatal embryonic hemorrhage in mice lacking core 1-derived O-glycans. *J Cell Biol* 2004; 164: 451-459.

Possible signaling pathways/relationships for the genes listed in “Bioinformatic analysis”, those listed in Supplemental table IV, plus selected genes listed in Supplemental table III. These genes and mechanisms are highlighted in yellow

For the first two statements below (•), see: references 15 and 35 in the paper, references given in Supplemental Table IV, and Red-Horse K, Das S. New research is shining light on how collateral arteries form in the heart—a future therapeutic direction? *Curr Cardiol Rep* 2021 2; 23: 30-34. For the third statement see Sox13 in “Bioinformatic analysis” and Olsen JJ, Pohl SÖ, Deshmukh A, Visweswaran M, Ward NC, Arfuso F, Agostino M, Dharmarajan A. The role of Wnt signaling in angiogenesis. *Clin Biochem Rev* 2017; 38: 131-142. For the remaining statements, see “Bioinformatic analysis”. *, See “Bioinformatic analysis” per context-dependent effects.

- **Low O₂** (Hypoxia) in watershed/collateral zone between arterial trees → **Egln1** → Hif → **VEGFA** → **Flk1** → **Rabep2**; **synectin**, **Notch1**, **DLL4**, **ADAM10/17**, **EphA4**, **Clic4**, **Gja4**, **CXCL12/SDF1** → **CXCR4** → Collaterogenesis (**Cgsis**); Hypoxia → **Rabep2** expression
- Fluid shear stress (disturbed/oscillatory; laminar/unidirectional) → eNOS → NO → Cgsis; Fluid shear stress → **EphrinB2/DLL4/KLF2** → Cgsis
- **Sox13** -- | **Wnt2** → β-Catenin → Angiogenesis (**AN**) → Cgsis (“AN/Cgsis” as denoted below, ie, certain known AN factors/mechanisms—yet to be confirmed—may contribute to Cgsis)
- **Cyb5r1** -- | Hypoxia → Hif → VEGFA → etc → Cgsis
- ***Rgs1** -- | GPCRs → G_α → AN; Ligand → GPCRs known to be involved with Cgsis: **CXCL12** → **CXCR4**, **Fractalkine** → **CX₃CR1** (**ADAM10/17** cleave membrane Fractalkine to soluble form), **S1P** → **S1PR1**, **MCP1** → **CCR2**
- **Fractalkine** → **CX₃CR1** → **IL1β**, **IL6**, **TNF_α** expression → autorelease of **MCP1** → inflammatory phenotype of hemopoietic/stem/progenitor cells → Cgsis
- Hypoxia → Hif → **Jak3**/STAT → VEGFA and several other angiogenic factors → Cgsis
Jak3 → β-Catenin → Adherens junctions → AN/Cgsis
Jak3 → bone marrow egress, homing and inflammatory phenotype of hemopoietic/stem/progenitor cells → Cgsis; ditto **MCP1** → **CCR2** → bone marrow...
- ***Yjfn3** → AN/Cgsis
- **Cav2** → αVβ3 integrin → Rac → AN/Cgsis
- **Cav2** → STAT3 → AN/Cgsis
- **Cav2** → eNOS → NO → Cgsis
- **Cav2** → G_α → Cgsis
- **Cav2** → TGF-β → Smad2/3 → AN/Cgsis
- **VEGFA** → **Flk1** → **Pld1** → PI3K-Akt, MEK/ERK → AN/Cgsis
- **Fat4** → pericyte differentiation → AN/Cgsis
- **Arhgap28** → RhoA → Endothelial cell lumenization → AN/Cgsis
- **Myom1** → αVβ3 integrin → Cgsis
- **Hif1_α** → **Tspyl2** -- | NFκB → VEGFA → Cgsis
- **TGFβ** → **Tspyl2** → AN/Cgsis
- **Tspyl2** → PI3K-Akt → AN/Cgsis
- **Foxr2** → Shh, ZO-1, Claudin5 → AN/Cgsis
- **C1galt1** → AN/Cgsis